

REPORT DOCUMENTATION PAGE

AFRL-SR-BL-TR-98-

0497

sources,
t of this
efferson

Public reporting burden for this collection of information is estimated to average 1 hour per response, inc
gathering and maintaining the data needed, and completing and reviewing the collection of information.
collection of information, including suggestions for reducing this burden, to Washington Headquarters Se,
Davis Highway, Suite 1204, Arlington, VA 22202-4302, and to the Office of Management and Budget, Paperwork Reduction Project

1. AGENCY USE ONLY (Leave blank)		2. REPORT DATE May 15, 1998		3. REPORT TYPE AND DATES COVERED Final Technical Report 01 Mar 95 to 28 Feb 98	
4. TITLE AND SUBTITLE ORGANIC POLLUTANTS IN SOILS, AS STUDIED BY NUCLEARMAGNETIC RESONANCE				5. FUNDING NUMBERS F49620-95-1-0192	
6. AUTHOR(S) Gary E. Maciel Willard L. Lindsay					
7. PERFORMING ORGANIZATION NAME(S) AND ADDRESS(ES) Department of Chemistry Colorado State University Fort Collins, CO 80523				8. PERFORMING ORGANIZATION REPORT NUMBER	
9. SPONSORING/MONITORING AGENCY NAME(S) AND ADDRESS(ES) AFOSR/NA 110 Duncan Avenue, Ste B115 Bolling AFB, DC 20332-8050				10. SPONSORING/MONITORING AGENCY REPORT NUMBER F49620-95-1-0192	
11. SUPPLEMENTARY NOTES					
12a. DISTRIBUTION AVAILABILITY STATEMENT Approved for public release; distribution unlimited.					
13. ABSTRACT (Maximum 200 words) This three-year project focussed on the development and application of state-of-the art NMR (nuclear magnetic resonance) techniques to elucidate the fundamental behaviors of certain organic pollutants (e.g., benzene, CCl, trichloroethylene, ethylene glycol) when adsorbed in typical soils, as represented in most of this study by the following major soil components: humics (humic acid, fulvic acid, humin), clays (montmorillonite, kaolinite) and silica. The first stage was the isolation/separation and detailed ¹³ C NMR characterization of the humic materials from a soil of southwestern Colorado; this work is resulting in the most detailed chemical-structural elucidation ever carried out on such a three-component humic suite. ¹³ C NMR studies revealed a spectacular case of co-contamination in reactions between CCl ₄ and benzene adsorbed in montmorillonite clays, yielding such Friedel-Crafts products as benzophenone, benzoic acid and (C ₆ H ₅) ₃ C ⁺ (the last being analogous to the product in a "ship-in-a-bottle" reaction between the two initial components in HY zeolite). ¹³ C NMR also elucidated the photo-assisted decomposition of trichloroethylene adsorbed on soil components (forming Cl ₂ CHCO ₂ H, Cl ₃ CCO ₂ H, Cl ₃ CCHCl ₂ , etc.), a much slower analog of the well-known conversions employing TiO ₂ (s) as the adsorbent. ² H NMR lineshape studies elucidated the detailed local motions of benzene, trichloroethylene and ethylene glycol adsorbed on major soil components.					
14. SUBJECT TERMS				15. NUMBER OF PAGES	
				16. PRICE CODE	
17. SECURITY CLASSIFICATION OF REPORT Unclassified		18. SECURITY CLASSIFICATION OF THIS PAGE Unclassified		19. SECURITY CLASSIFICATION OF ABSTRACT Unclassified	
				20. LIMITATION OF ABSTRACT UL	

19980617 029

22 MAY 1998

FINAL TECHNICAL REPORT

ORGANIC POLLUTANTS IN SOILS, AS STUDIED BY NUCLEAR MAGNETIC RESONANCE

Gary E. Maciel
Department of Chemistry
Colorado State University
Fort Collins, CO 80523

Willard L. Lindsay
Department of Agronomy
Colorado State University
Fort Collins, CO 80523

Grant No. F49620-95-1-0192

Performance Period: March 1, 1995 – February 28, 1998

Objectives

The goal of this project was to elucidate as much detail as possible regarding the chemical/physical behaviors of certain organic pollutants (e.g., benzene, ethylene glycol, trichloroethylene and fluorocarbon ethers) in soils, initially in terms of primary soil constituents, i.e., humic acids, fulvic acids and clays (kaolinite and montmorillonite). This study was designed to provide the kind of fundamental chemical/physical information that can be used by others for constructing models of the sequestering, decomposition and transport of organic pollutants and their residues in soil/groundwater systems. Because of time constraints, work on the fluorocarbon ethers was only minimal, and will not be discussed in this report.

Organization of the Effort

The primary tool of this study was nuclear magnetic resonance (NMR), employing detection of primarily the nuclides, ^1H , ^2H , ^{13}C , ^{19}F , ^{27}Al and ^{29}Si . Both liquid solutions (e.g., pollutant + humic or fulvic acid) and solid samples (e.g., pollutant/clay or pollutant/humic "complex") were studied by high-resolution NMR techniques. Emphasis was heavily on the latter. Magnetic fields ranging from 2.1 T (90 MHz proton resonance frequency) to 14 T (600 MHz proton frequency) were employed.

DTIC QUALITY INSPECTED 1

This report is organized primarily on the basis of providing a relatively detailed description of each major aspect of the project. In several cases, the data resulted in manuscripts that have been published, accepted or submitted for publication, or are at the stage of a draft of a manuscript being revised to submit for publication. In most of those cases, copies of the manuscripts are included as part of this report, and the work is described only briefly elsewhere in the report; in cases where a manuscript is in preparation, but is not quite ready at this time, the manuscript(s) will be provided upon request.

This project focused on the development and application of multinuclear NMR strategies for elucidating the fundamental physical/chemical (*abiotic*) behaviors (chemical reactions, interactions, local mobilities) of specific organic pollutants in major soil components (clays, silica and humic materials – humic acid, fulvic acid, humin) and, to a lesser degree, whole soils. This overall effort, and this report, can be viewed in terms of the following separate, but related, theme areas: 1) choosing and characterizing the clays to be used for pollutant/clay studies; 2) isolation and characterization of humic materials for pollutant studies; 3) local mobilities of certain organic pollutants adsorbed on/in soil components; 4) photo-assisted decomposition of $\text{Cl}_2\text{C}=\text{CHCl}$ adsorbed on soil components; 5) co-contamination of zeolites and clays with CCl_4 and benzene; and 6) the silica surface.

Accomplishments/New Findings

1. *Clays.* One of the important tasks of the first several months of this project was selecting and characterizing suitable clay and humic materials on which to base the pollutant/soil system samples and studies. The clays that were ultimately selected, based on x-ray powder diffraction, elemental analysis and ^{29}Si and ^{27}Al NMR data, are a kaolinite and a Ca-montmorillonite obtained from the Missouri Clay Repository, Columbia, MO. Figures 1-3 show ^{27}Al and ^{29}Si NMR spectra of these clay samples, based on magic angle spinning (MAS) and, in the ^{29}Si spectra, either direct polarization (DP, generation of ^{29}Si spin polarization directly by ^{29}Si spin-lattice relaxation) or cross polarization (CP, a transfer of spin polarization from protons to ^{29}Si nuclei, based on the existence of strong, static components of ^1H - ^{29}Si magnetic dipole-dipole interactions).

In the ^{27}Al NMR spectra shown in Figure 1, one sees the expected dominance of the octahedral (O_h) peak at about 0 ppm and a much smaller tetrahedral (T_d) aluminum peak at about 50-60 ppm, the latter representing a small, but significant quantity of Al-for-Si substitutions in the tetrahedral (nominally silicon) planes of the clay structures. In the ^{29}Si NMR spectra of Ca-montmorillonite (Fig. 2) and kaolinite (Fig. 3), one sees the strong tetrahedral silicon peak expected for clay structures. For the Ca-montmorillonite, there is also a small peak at about -110 ppm, due to silica. The fact that this peak shows up so strongly in the CP spectrum, where the observed ^{29}Si spin polarization has been transferred from protons (presumably in either surface SiOH groups or physisorbed H_2O), implies a higher surface areas than one would expect for the quartz-like silica normally assumed to be present in soils. The fact that metal ion exchange with Cu^{2+} enhances the relative intensity of the silica peak of Ca-montmorillonite (Fig. 4), along with broadening both peaks (as expected for a paramagnetic agent), indicates that the added Cu^{2+} is incorporated into, or complexed with, both the clay and the silica; this observation may represent an important step in elucidating the true nature of this silica.

The humic samples on which much of this project is being based were isolated from a soil that we collected in the Uncompahgre National Forest of southwestern Colorado. The classical soil separation procedures yielded humic acid, fulvic acid and humin fractions, for which the ^{13}C CP-MAS NMR spectra are shown in Figure 5, which also provides structural assignments for the major peaks and shoulders.

2. Humic Materials. This aspect of the project, which we had expected be completed shortly after the first year of the project, has turned out to be a much bigger, and much more important, task than we had envisioned. This work is now nearly complete and a full paper on it will be submitted shortly. After we learned that commercially available humic materials are either not available in sufficient quantities to support our program (e.g., samples from the International Humic Substances Society) or of questionable origin and significance (e.g., from Aldrich), we decided to collect our own soil and perform the separations into humic acid, fulvic acid and humin, based on the classical acid/base dissolution procedures. This approach also offered the prospect of obtaining the three types of samples from *one* soil source, so the suite of three materials will have maximum significance to soil scientists and organic geochemists. Since we were choosing the soil ourselves, we were free to choose one that has a low-iron

content, minimizing the NMR complications that one encounters from paramagnetic and ferromagnetic iron sites in a soil. We collected a soil from the Uncompahgre National Forest of southwestern Colorado, about 18 inches below the "leaf litter." The "classical" (wet chemical) characteristics were also measured for this soil.

The ^{13}C CP-MAS spectra of the whole soil and the three solid organic components that we separated from it are shown in Figure 5. Shown with the spectra are peak assignments based on chemical shifts of known chemical functionalities and on spectral editing (*vide infra*). One sees a wide variety of organic chemical functionalities in these humics, making them ideal for the pollutant/soil interaction studies of this project. One notes the close match-up between the computer-synthesized spectrum of Fig. 1e (a linear combination of the spectra of humic acid, fulvic acid and humin) and the spectrum of the whole soil, indicating that any chemical changes that occurred in the chemical structures of the organic soil components during the acid/base separation procedure are minimal or subtle. Figure 6 shows the liquid-sample ^{13}C NMR spectrum of the fulvic acid component. Its improved resolution, relative to that of the CP-MAS spectrum of Fig. 1d, is due primarily to the averaging by liquid-state motion of small differences in isotropic chemical shifts (due to corresponding small differences in local geometry, e.g., conformation) for each particular class of functional group.

In order to identify, or confirm, the chemical structure(s) responsible for each spectral region of the spectra shown in Figure 5, spectral editing experiments were carried out. The most primitive of these techniques is the popular "interrupted-decoupling" or "dipolar-dephasing" technique, which differentiates between $-\text{CH}_2-$ or C-H groups and $-\text{CH}_3$ or CH_0 groups in terms of their behaviors under a period during which the ^1H decoupler is turned off. From the dipolar-dephasing spectra on the three humic samples, shown in Figure 7, one can make the structural distinctions indicated above.

A higher level of spectral editing, distinguishing among the four carbon types, CH_3 , CH_2 , CH and CH_0 (no directly attached hydrogens) is achievable, at great cost in spectrometer time, by the combination of CP experiments, including cross depolarization, developed by Zilm and Wu and co-workers. These techniques have been applied to the three humic materials of this study. Figure 8 shows the individual component spectra, derived after the appropriate combinations of spectra obtained according to the published approach, and the composite spectra obtained by addition of

these components. Figure 9 shows the general procedure used for spectral editing.

In addition to applying published spectral editing methods, we attempted unsuccessfully to develop an alternate method, based on increasing T_{2C} sufficiently (at lower temperatures) to permit J_{CH} -based spectral editing, in direct analogy to what is done routinely on liquid samples. Although continued work on the structural characterization of humic materials is not now a major issue in a renewed project, we plan to see if an improved ^{13}C spectral-editing technique can be based on a *synchronized combination* of MAS with a suitable multiple-pulse sequence.

In order to quantitate the intensities of the various spectral regions assigned by the combination of chemical shift recognition and spectral editing, we carried out spin counting experiments on the three humic samples of this study. For this purpose, DP-MAS experiments (**d**irect **p**polarization, no CP) were carried out, based on long repetition delays (4s) and relaxation corrections computed from ^{13}C T_1 values that we had determined. Quantitation in corresponding CP-MAS experiments was achieved by variable contact-time determinations (Figures 10-12) of the CP-relevant relaxation parameters. In the quantitation experiments, a previously developed ^{13}C -labeled bicyclic ketone (labeled carbonyl peak outside the main spectral region of these humic samples) was contained in a small capillary as an intensity reference. Figure 13 shows typical high-S/N, CP-MAS and DP-MAS spectra obtained for this purpose, showing the T_{1C} values and relative populations for each indicated region of the spectrum.

^{13}C CP-MAS and DP-MAS spectra we have obtained on the Uncompahgre humic samples (e.g., Figure 13) have unusually and remarkably high quality. We do not believe that spectra of this quality have been obtained by any other laboratory on humic samples. With such high quality (e.g., high S/N), it is possible to extract substantial structural detail via spectral deconvolution. Figure 14 shows pictorially the results of one such analysis.

The spectral editing and spin counting experiments described here are now being completed on the humin sample. These data are being interpreted in terms of hypothetical structural models. Before submitting the paper on this study (probably about June, 1998), we will have elucidated more detailed structural knowledge (both qualitative and quantitative) about the

organic components of Uncompahgre soil than has ever been available previously on *any* soil.

3. *Mobilities of Adsorbed Organic Pollutants.* Another productive strategy of this project was the application of ^2H NMR lineshapes of deuterium-labeled organics adsorbed on/in major soil components. To various levels of detail and completeness, a series of pollutant species were examined in this manner. These include $\text{HOCD}_2\text{CD}_2\text{OH}$, benzene (C_6D_6) and $\text{Cl}_2\text{C}=\text{CDCl}$. The overall strategy was to obtain ^2H lineshapes, which are dominated by deuterium's orientation-dependent nuclear electric quadrupole interaction, as a function of temperature, and then try to model each line shape with computer-simulated line shapes based on specific motional models for the C-D moiety. From these comparisons, one can usually elucidate the detailed nature of motion at each temperature (from which an activation energy can also be obtained).

Our most detailed ^2H lineshape study has been on ethylene glycol (used heavily in aircraft de-icing), for which a detailed paper is in preparation, describing the dependence of the motion of ethylene glycol adsorbed on/in a Ca-montmorillonite clay as a function of loading level, water content and metal-ion exchange. Figure 15 shows a representative set of ^2H spectra measured from -125°C to 30°C , which show a general narrowing and change in line shape as the sample temperature was increased. Figure 16 shows the computer-generated lineshape simulations that correspond to the experimental spectra of Fig. 15; these simulations were based on a simulation model in which the C-D moieties are exchanging between two populations. In one population the C-D bond reorients (essentially isotropically) among the positions corresponding to the twelve vertices of an icosahedron; in the other population, the C-D moieties occupy (randomly) just one orientation. The populations and exchange rates of these simulations are listed in Figure 16.

An analogous analysis has been carried out for ethylene glycol adsorbed on humic acid (Figure 17) and on a whole soil. Manuscripts based on these results are currently being prepared for publication.

^2H NMR lineshape studies were carried out on benzene adsorbed on Ca-montmorillonite at different loading levels and clay-moisture contents. Figures 18 and 19 display representative spectra. Simulations (not given here) show that the benzene molecules in these systems manifest, at

temperatures above the melting point of benzene, higher levels of local mobility than seen for samples with polar functional groups. These results have been described in a manuscript submitted for publication.

A few ^2H NMR lineshape experiments have also been carried out on $\text{Cl}_2\text{C}=\text{CDCl}$ adsorbed on Ca-montmorillonite. Figure 20 shows representative spectra. These results have been included in a manuscript submitted for publication.

4. *Photo-Assisted Decomposition of Trichloroethylene Adsorbed on Soil Components.* This work has been described in detail in a manuscript that has been submitted for publication. Only a few highlights are described here.

The general focus in this specific theme area was to begin characterizing the photo-induced chemistry that occurs with chlorohydrocarbons at the air/soil interface. This focus is in contrast to the huge literature that already exists on the photo-induced decomposition of chlorohydrocarbons in model reactors designed for the clean-up of waste water. Apparently the most successful photochemistry-based remediation systems rely on $\text{TiO}_2(\text{s})$ as a substrate. Our work was directed to substrates that are highly abundant in soils, e.g., (especially) clays, silica and humics.

Our ^{13}C NMR-based study has shown that trichloroethylene adsorbed on a variety of substrates (clay, silica, humic acid) decomposes to a variety of products (e.g., $\text{Cl}_2\text{CHCO}_2\text{H}$, $\text{Cl}_3\text{CCO}_2\text{H}$, $\text{Cl}_3\text{CCHCl}_2$, OCCl_2 and CO_2) under the influence of long-wavelength UV radiation, over a period of a few hours to several days. Figure 21 shows the ^{13}C MAS spectra obtained on $\text{Cl}_2\text{C}=\text{CHCl}$ /Ca-montmorillonite samples subjected to near-UV irradiation over periods of up to 20 days. As indicated on the figure, all of the above-mentioned decomposition products can be seen in the ^{13}C DP-MAS spectra, except the most volatile components, CO_2 and Cl_2CO (phosgene), which escape the reaction cell. After 10-20 days, most of the components are gone from the spectrum, largely decomposed to gaseous products (which we quantitated by using suitable collection traps). Figure 22 shows that this behavior is not specific to Ca-montmorillonite; analogous behaviors, albeit different in detail, are observed with a variety of other soil-based substrates (i.e., ion-exchanged montmorillonites, kaolinite, silica, humic acid and soil).

At this stage we have considerable detail on the photochemically-assisted product formation and product distribution for $\text{Cl}_2\text{C}=\text{CHCl}$ /Ca-

montmorillonite, almost no such details for $\text{Cl}_2\text{C}=\text{CHCl}$ adsorbed on any other substrate, and no information on the corresponding photophysics of any of these processes. These are areas that we propose to research as a major part of a subsequent project.

5. *Co-Contamination with Benzene and CCl_4 Adsorbed on Clays and Zeolites.* This aspect of our project has been described in two publications. Therefore, again, only highlights are described here.

Our first hint of “co-contaminant chemistry” came with the observation that $(\text{C}_6\text{H}_5)_3\text{C}^+$ carbenium ions could be generated inside the cavity of HY zeolite, from a mixture of benzene and CCl_4 . These carbocations are presumably formed by chemical processes of the Friedel-Crafts variety inside the zeolite cavities in a kind of “ship in a bottle” synthesis (Fig. 23). That the carbocations were formed *inside* the zeolite, rather than on the outer surfaces of the zeolite particles, was demonstrated by chemical responses of the “trapped” $(\text{C}_6\text{H}_5)_3\text{C}^+$ species to reagents of various diagnostic sizes. Figure 24 shows the ^{13}C NMR evidence for the formation of the $(\text{C}_6\text{H}_5)_3\text{C}^+$ ions. Supporting evidence on the motional characteristics of $(\text{C}_6\text{H}_5)_3\text{C}^+$ cations inside the zeolite cavities, or adsorbed on the outside particle surfaces, was provided by ^2H NMR results. Figure 25 shows representative ^2H NMR lineshapes for a sample containing $(\text{C}_6\text{H}_5)_3\text{C}^+$ inside zeolite cavities; computer simulations of the ^2H lineshape (not given here) show that this species executes a type of motion that is analogous to that of a constrained, but isotropically reorienting, species.

Based on the provocative results described briefly above on the Friedel-Crafts chemistry occurring in HY zeolite between two important pollutants (C_6H_6 and CCl_4), and recognizing the catalytic similarities between certain zeolites and certain clays, we examined the $\text{CCl}_4/\text{C}_6\text{H}_6$ system in clay samples. Figure 26 shows ^{13}C CP-MAS and DP-MAS spectra of CCl_4 , benzene and the $\text{CCl}_4\text{-C}_6\text{H}_6$ combination adsorbed on Ca-montmorillonite, Zn^{2+} -exchanged montmorillonite, kaolinite, Zn^{2+} -exchanged kaolinite and K-10 montmorillonite. One sees in Fig. 26 that, especially for the Zn^{2+} -exchanged montmorillonites, chemistry of the Friedel-Crafts type occurs in these clay systems. In these cases, in contrast, to the zeolite analog, other Friedel-Crafts products are formed, e.g., $\text{C}_6\text{H}_5\text{CO}_2\text{H}$ and $(\text{C}_6\text{H}_5)_2\text{CO}$.

6. *The Silica Surface.* A long-term theme in our research program has been the detailed characterization of structure, dynamics and chemical

reactivity at silica surfaces. Since these issues are *a priori* highly relevant to the subject of pollutant behaviors in soils, some attention has been directed in this project to NMR studies that focus on various characteristics of silica surfaces, especially the distribution and structural/ dynamical characteristics of silanols (SiOH groups) on the surface. In the early stages of this project we completed a detailed ^1H and ^{29}Si NMR study of fumed silicas, focusing on the differences and similarities between the fumed silica surface and that of silica gel. This work was described in detail in a paper published in *J. Am. Chem. Soc.*

In our latest publication on the silica surface (based, at least in part, on this project), we presented a generalized version of a previously suggested model of the silica surface, in which geminal silanols are situated on surface segments similar to (100)-type faces of the β -cristobalite structure and single silanols are situated on surface segments similar to corresponding (111)-type faces. This model was supported by an extensive body of spectroscopic data, especially our own ^{29}Si and ^1H NMR data, gathered over a period of roughly 15 years. In this model single silanols on the same (111)-type surface segment cannot form hydrogen bonds with each other. Whether or not adjacent geminal silanols on the same (100)-type surface segment can form hydrogen bonds with each other depends on the relative orientation of their hydroxyl groups. When two surface segments of either (100)-type or (111)-type intersect convexly, hydroxyl groups cannot participate in hydrogen bonding across the intersection; but when two surface segments intersect concavely, those silanols situated at the intersection can form hydrogen bonds with their counterparts across the intersection. All the hydrogen-bonding silanols in this generalized β -cristobalite model have a common feature: when any two silanols are hydrogen bonded to each other, the two silicon atoms containing them are also situated on the same (100)-type surface segment. The generalized β -cristobalite surface model can also explain the reversible dehydroxylation and rehydroxylation process on silica surfaces. Both single and geminal silanols participating in hydrogen bonding are most easily dehydroxylated under evacuation at temperatures between 170 and 450° C and form low-strain bicyclo[3.3.0]octasiloxane rings. The mode of dehydroxylation on a silica surface undergoes a transformation between 450 and 650° C, yielding highly strained trisiloxane rings for dehydroxylation at $T \geq 650^\circ\text{C}$, according to this model. We expect this model to prove useful in interpreting data of this project on the interactions of organic pollutants with silica.

Personnel Supported

Faculty: G.E. Maciel

Postdocs (partially supported): I.-S. Chuang, J. Xiong, J. Yang, H. Lock

Graduate Students: D. Keeler, T. Tao, C. Liu, M. Seger

Publications Citing Grant No. F49620-95-1-0192 (copies available on request)

Ting Tao and Gary E. Maciel, "¹³C NMR Observation of the Triphenylmethyl Cation Imprisoned in the Zeolite HY Supercage," *J. Am. Chem. Soc.*, **117**, 12889-12890, (1995).

Changhua Liu and Gary E. Maciel, "Structure of the Fumed Silica Surface: A Study by NMR," *J. Am. Chem. Soc.*, **118**, 5103 (1996).

I-Ssuer Chuang and Gary E. Maciel, "A Generalized β -Cristobalite Model of Silica Surfaces. Silanol Hydrogen Bonding and Surface Structure," *J. Phys. Chem.*, **101**, 3052-3064 (1997).

I-Ssuer Chuang and Gary E. Maciel, "Probing Hydrogen Bonding and the Local Environment of Silanols on Silica Surfaces via Nuclear Spin Cross Polarization Dynamics," *J. Am. Chem. Soc.*, **118**, 401-406 (1996).

Ting Tao and Gary E. Maciel, "¹³C NMR Study of Co-Contamination of Clays with Carbon Tetrachloride and Benzene," *Environ. Sci. Technology*, **32**, 350-357 (1998).

David Keeler, Jincheng Xiong and Gary E. Maciel, "The Local Mobility of Ethylene Glycol Adsorbed on Clay Substrates," *J. Phys. Chem.*, to be submitted.

Jincheng Xiong, Herman Lock and Gary E. Maciel, "Local Motion of Organic Pollutants in Soil Components, as Studied by ²H NMR," *Environ. Sci. Technol.*, submitted.

Ting Tao, Jane J. Yang and Gary E. Maciel, "Photo-Assisted Decomposition of Trichloroethylene on Clay," *Environ. Sci. Technol.*, submitted.

Jincheng Xiong, Ting Tao and Gary E. Maciel, "²H NMR Characterization of Motion and Mobility of Zeolite-Immobilized Triphenylmethyl Carbocations," *J. Phys. Chem.*, submitted.

Inventions/Patents

None

Acknowledgement/Disclaimer

This work was sponsored (in part) by the Air Force Office of Scientific Research, USAF, under grant number F49620-95-1-0192. The views and conclusions contained herein are those of the authors and should not be interpreted as necessarily representing the official policies or endorsements, either expressed or implied, of the Air Force Office of Scientific Research or the U.S. Government.

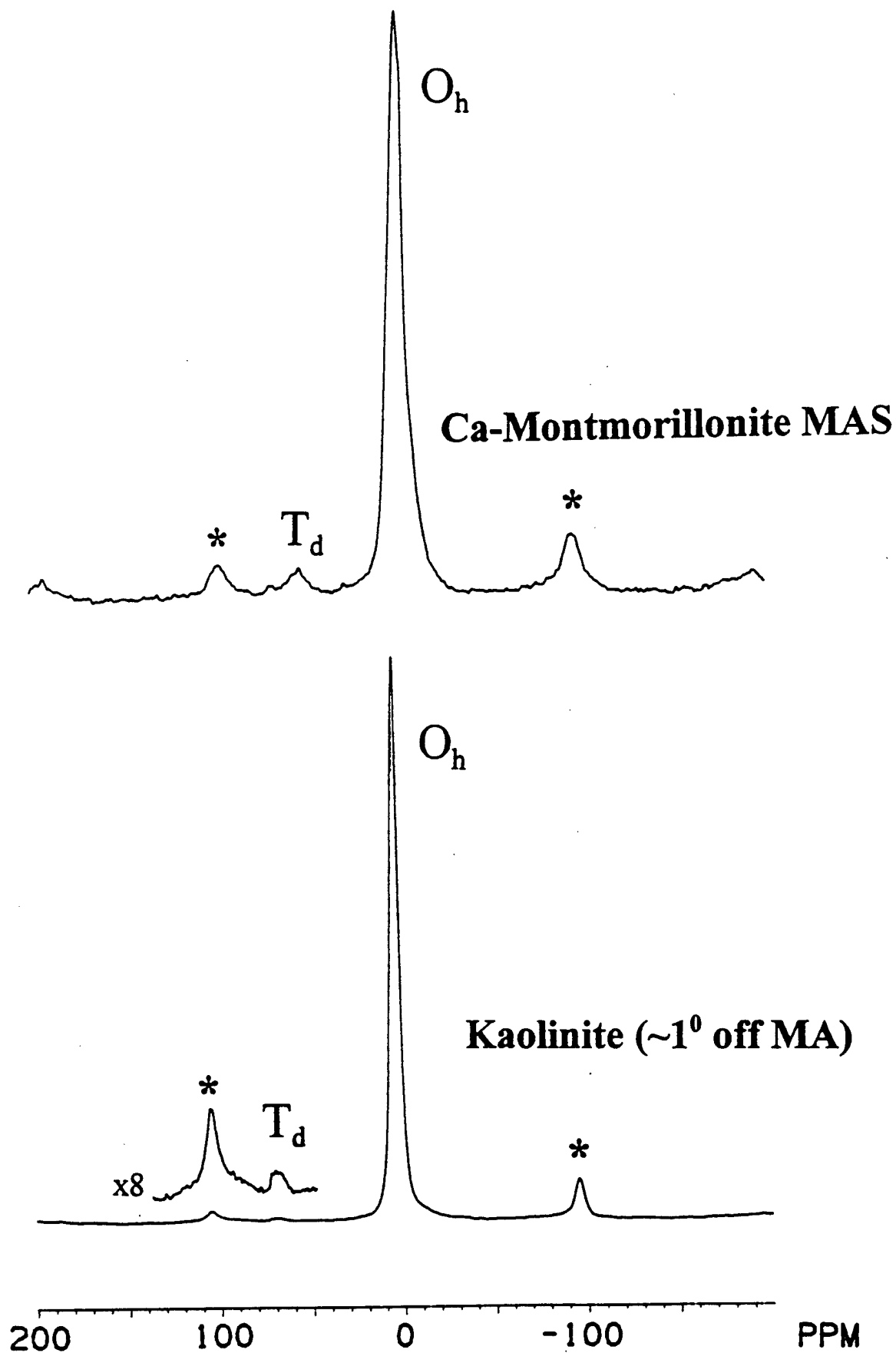


Figure 1. ^{27}Al MAS (magic-angle spinning) NMR spectra of clay minerals. Upper, Ca-montmorillonite. Bottom, kaolinite. T_d designates the tetrahedral site; O_h designates the octahedral site. Asterisks designate MAS sidebands.

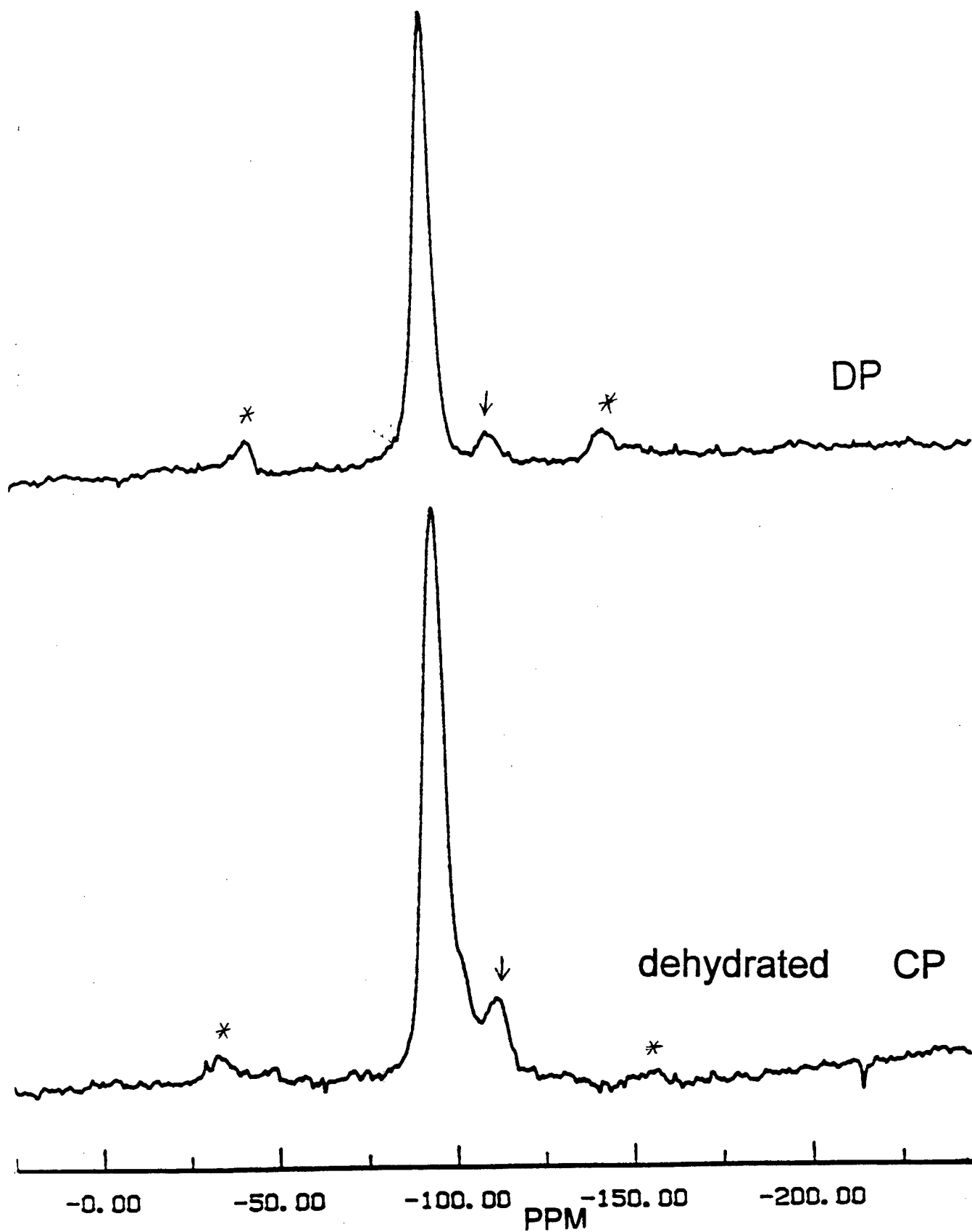


Figure 2. ^{29}Si MAS spectra of Ca-montmorillonite. Upper, DP (direct polarization). Lower, CP (cross polarization). Asterisks denote spinning sidebands. Arrow denotes silica peak.

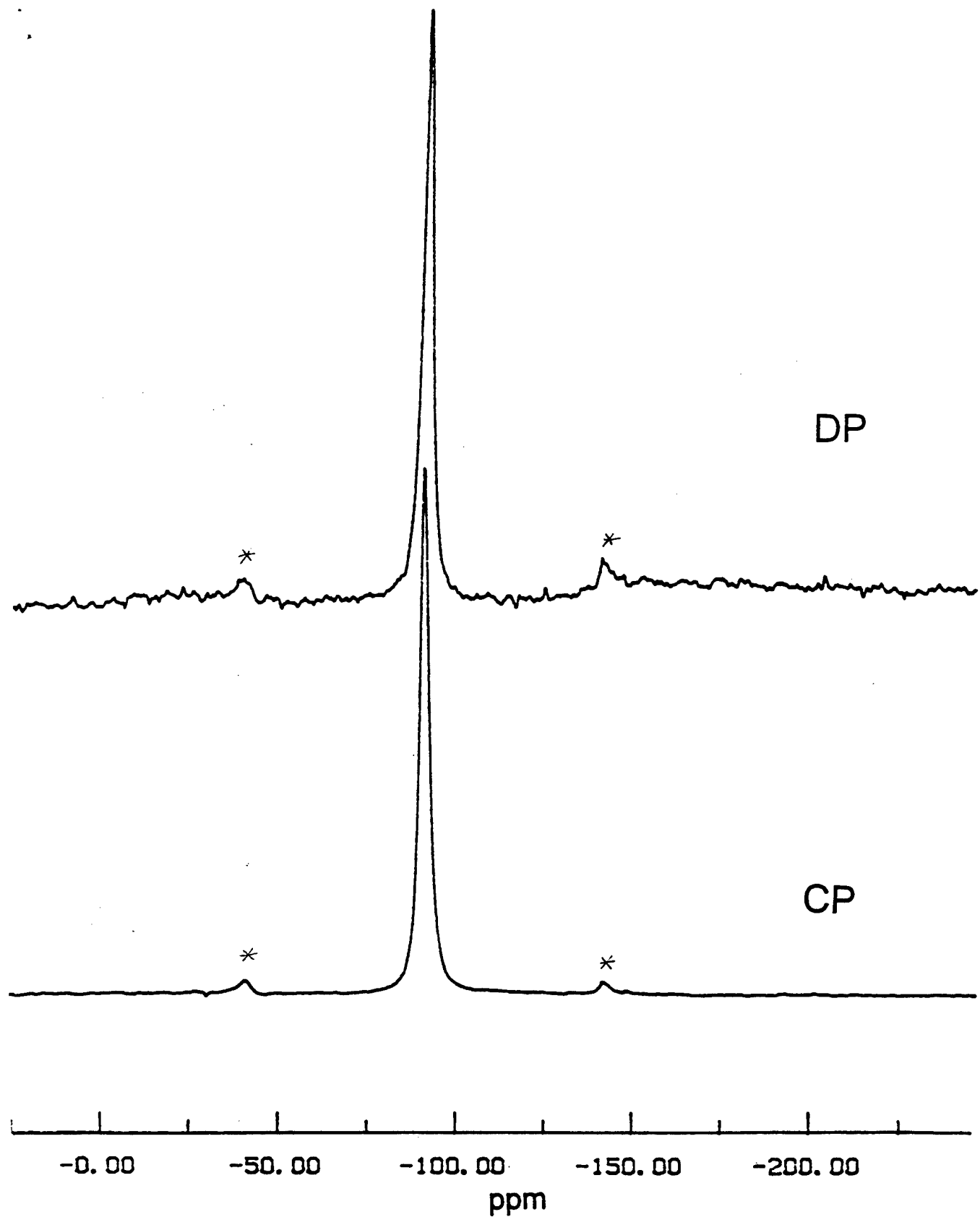


Figure 3. ^{29}Si MAS spectra of hydrated kaolinite. Asterisks denote MAS sidebands.

CP-MAS

DP-MAS

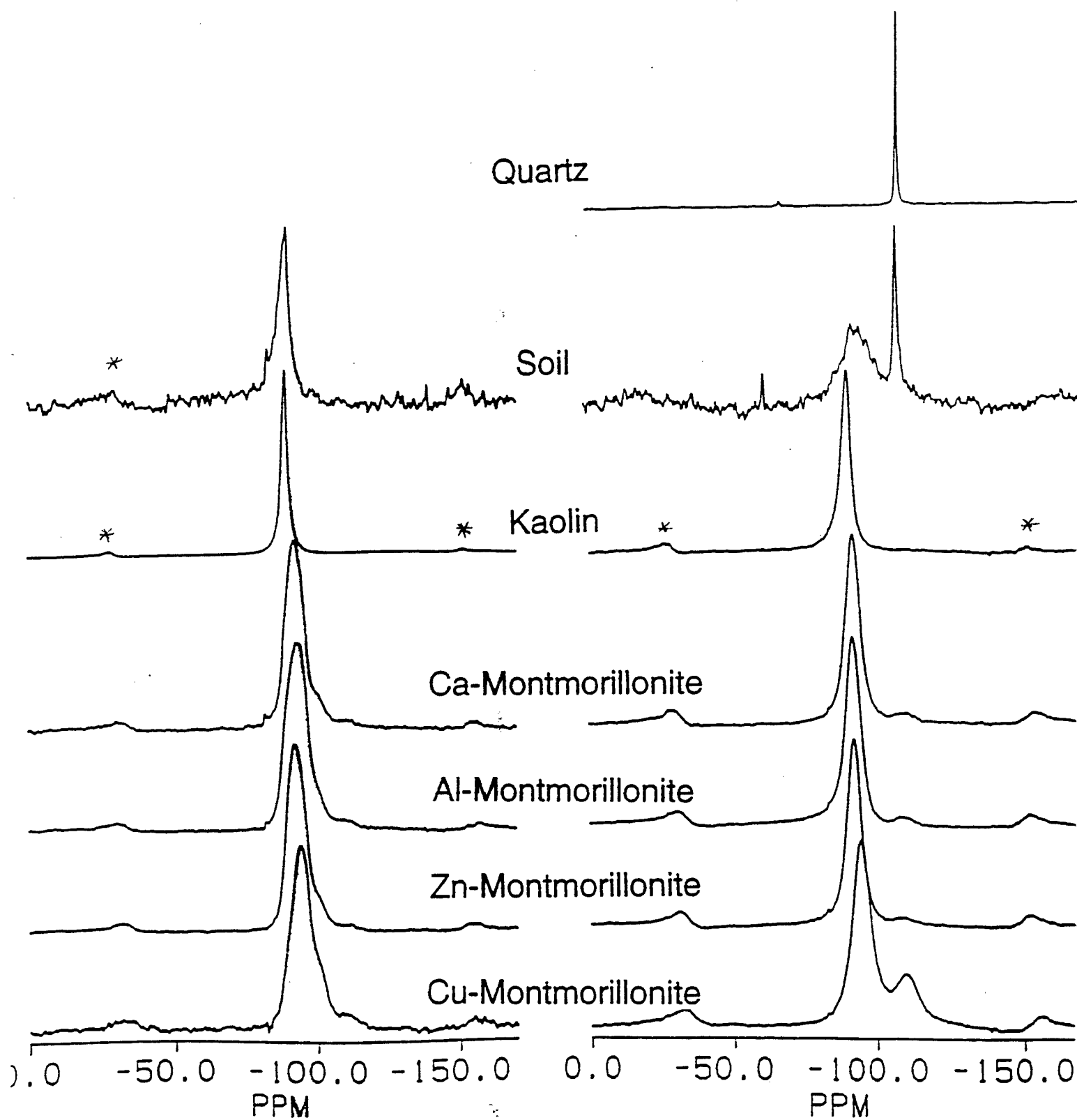


Figure 4. ^{29}Si MAS spectra of clays and soils. Asterisks denote MAS sidebands.

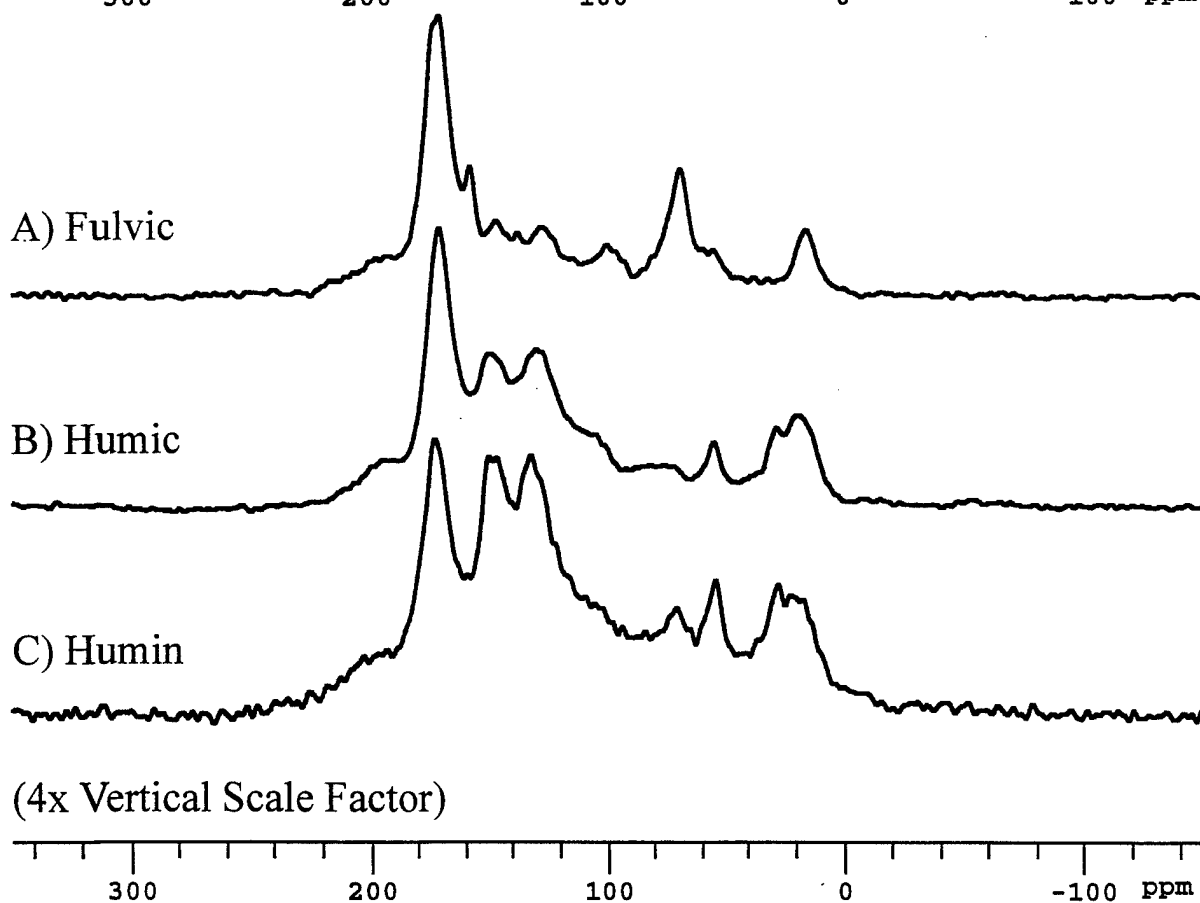
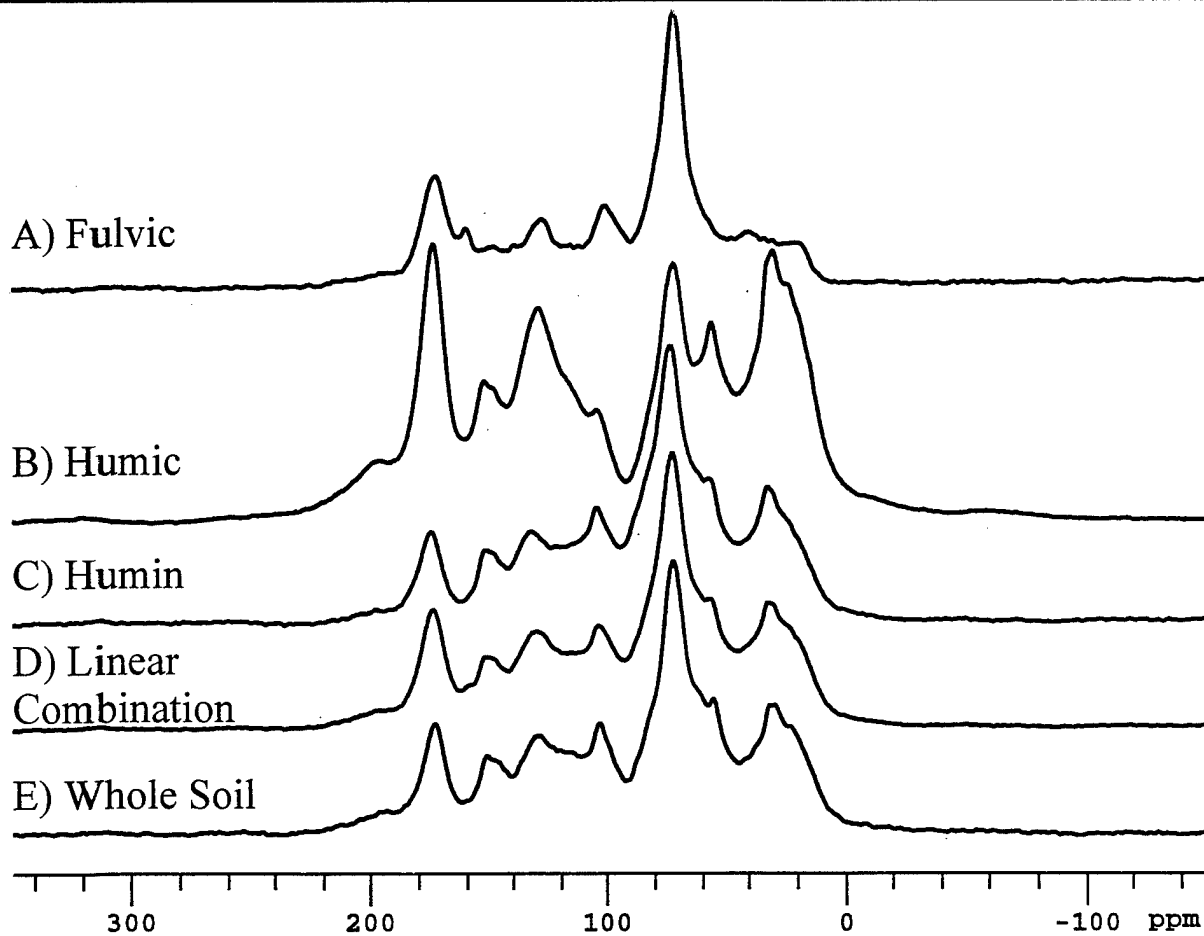


Figure 5. ^{13}C CP-MAS spectra of A) fulvic acid, B) humic acid, C) humin from the Uncompahgre National Forest and E) whole soil. D) Computer-generated linear combination spectrum: $(0.090)(1A) + (0.15)(1B) + (0.76)(1C)$.

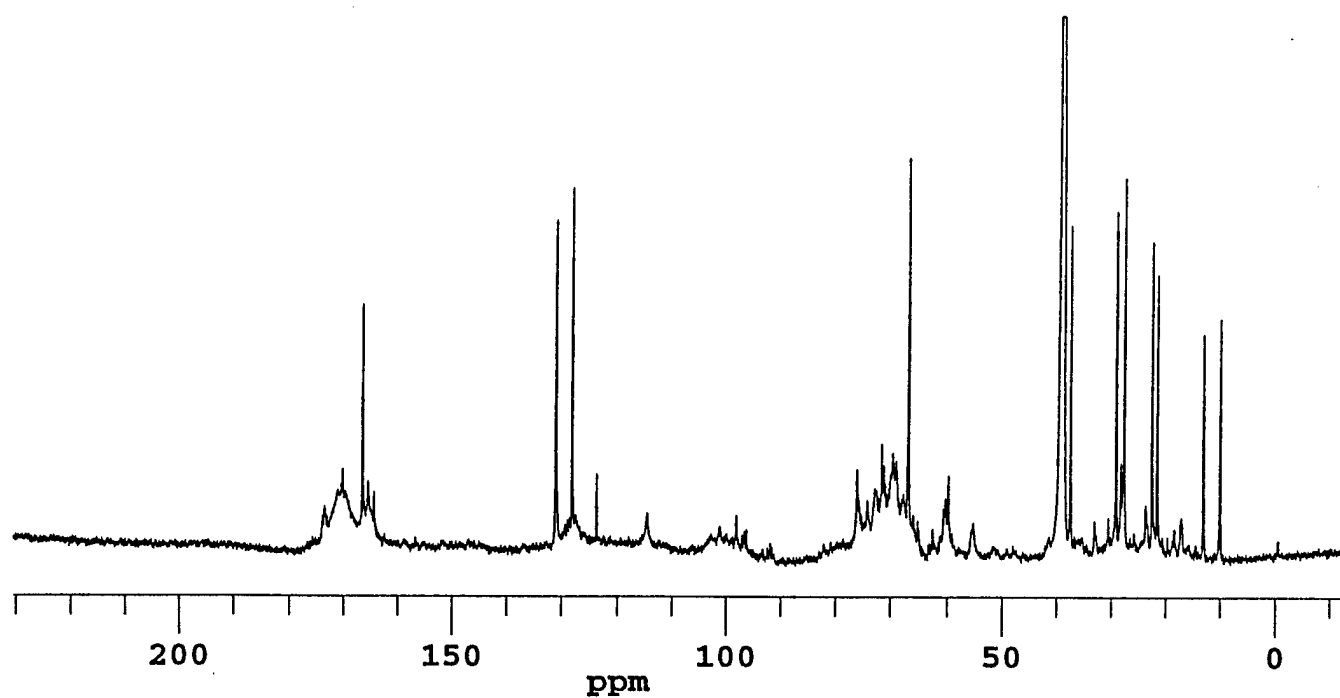


Figure 6. Liquid-solution ^{13}C NMR spectra of the Uncompahgre fulvic acid (in $(\text{D}_3\text{C})_2\text{SO}$).

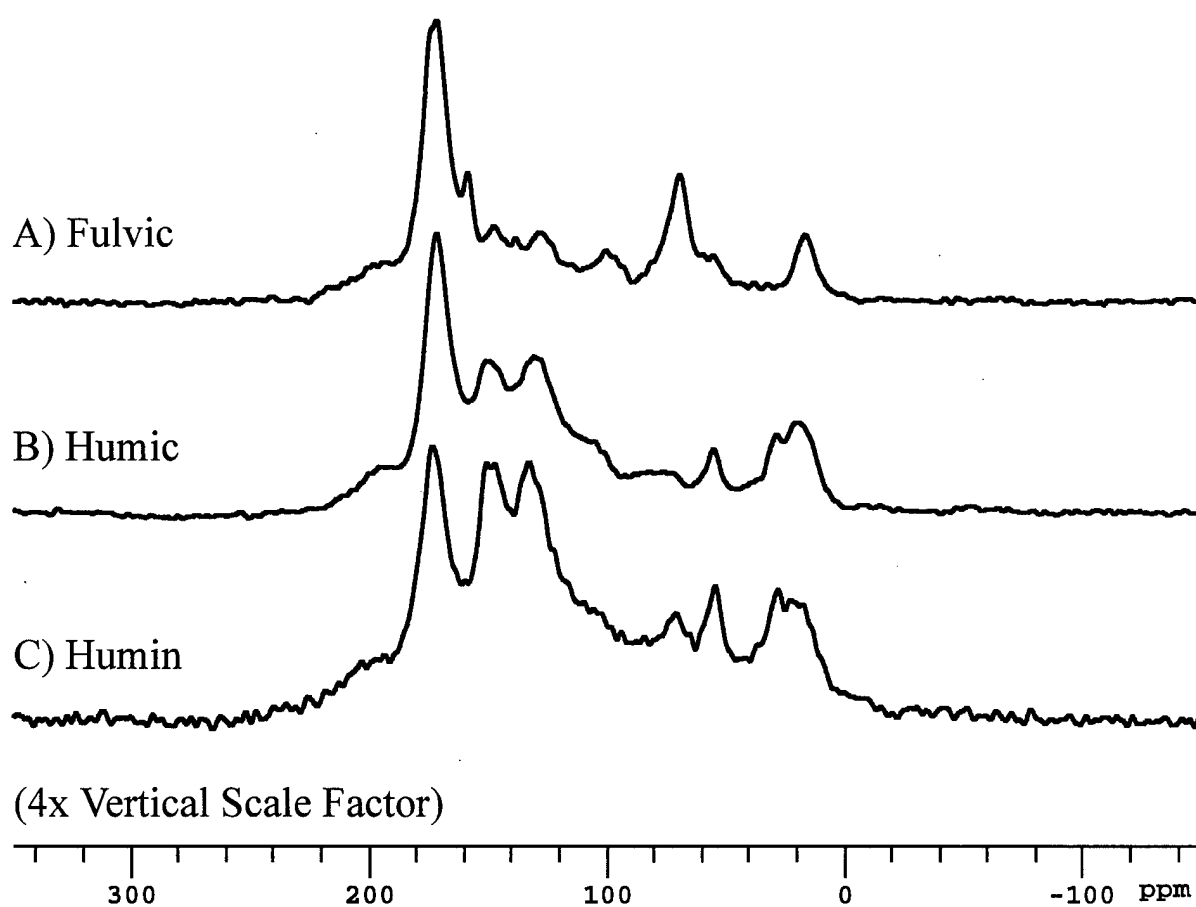


Figure 7. Dipolar-dephasing ^{13}C CP-MAS spectra of Uncompahgre fulvic acid (A), humic acid (B) and humin (C). 75 μs dipolar-dephasing period.

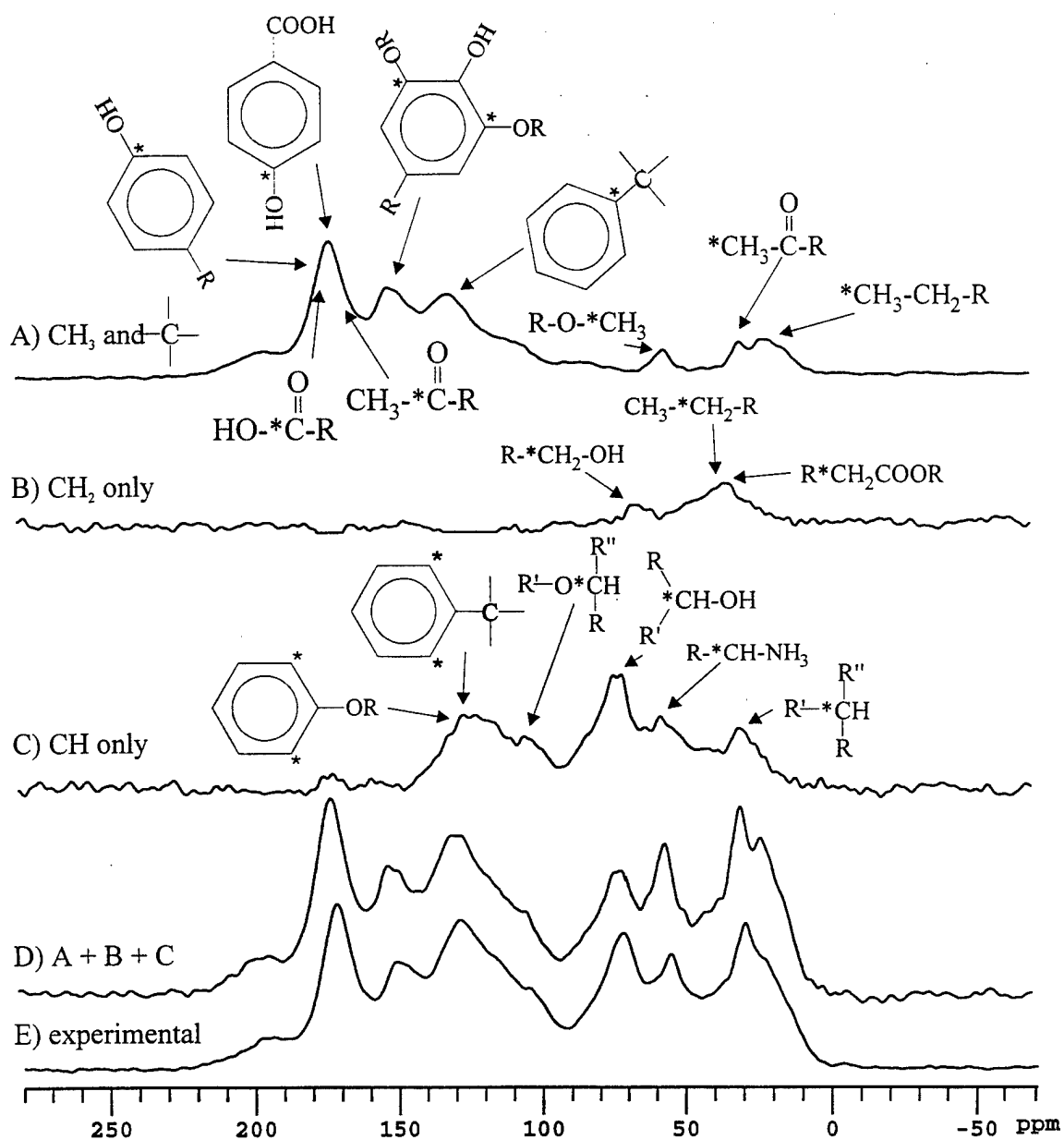
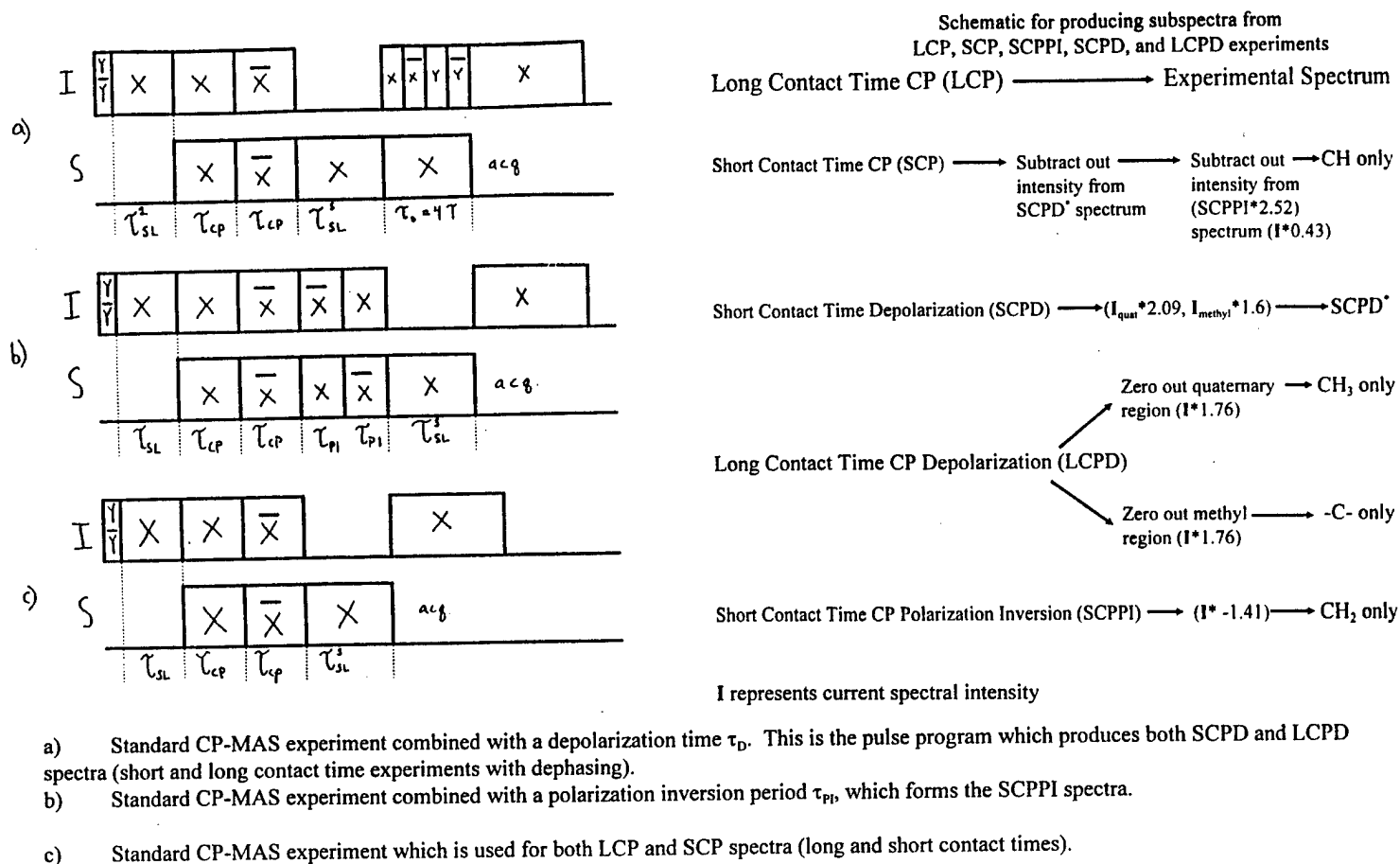


Figure 8. ^{13}C CP-MAS spectral editing of the Uncompahgre humic acid A) - C), individual component spectra derived according to the published method; D) Composite spectrum obtained from the individual components; E) Experimental CP-MAS spectrum (Fig. 1B).



X. Wu, S. Burns, and K. Zilm, *J. Magn. Reson. A* **111**, 29 (1994)

Figure 9. General procedure used for obtaining CP-based spectral editing of ¹³C NMR spectra of the type shown in Figure 8.

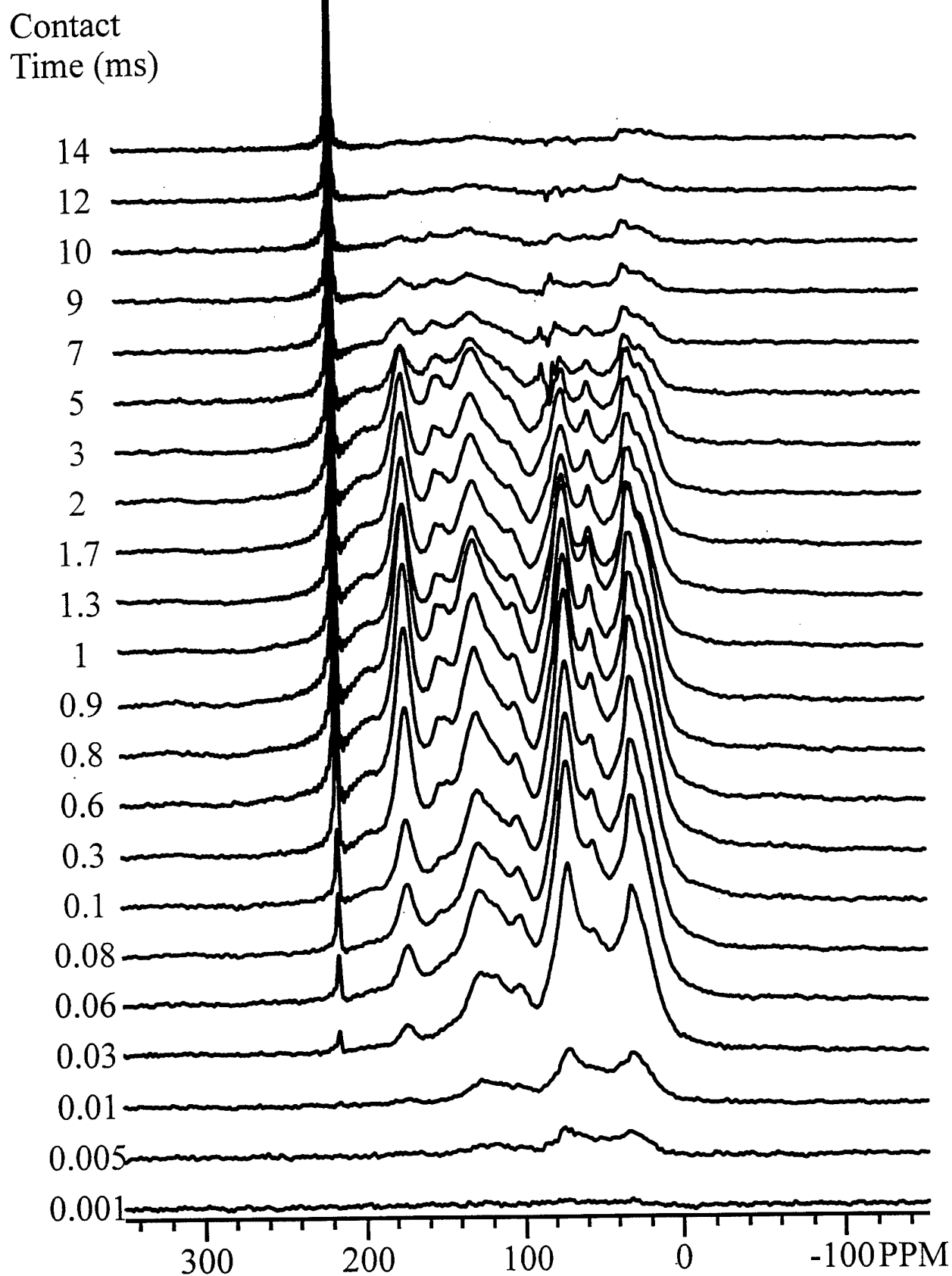


Figure 10. ^{13}C spectra of a variable contact-time CP-MAS experiment on Uncompahgre humic acid.

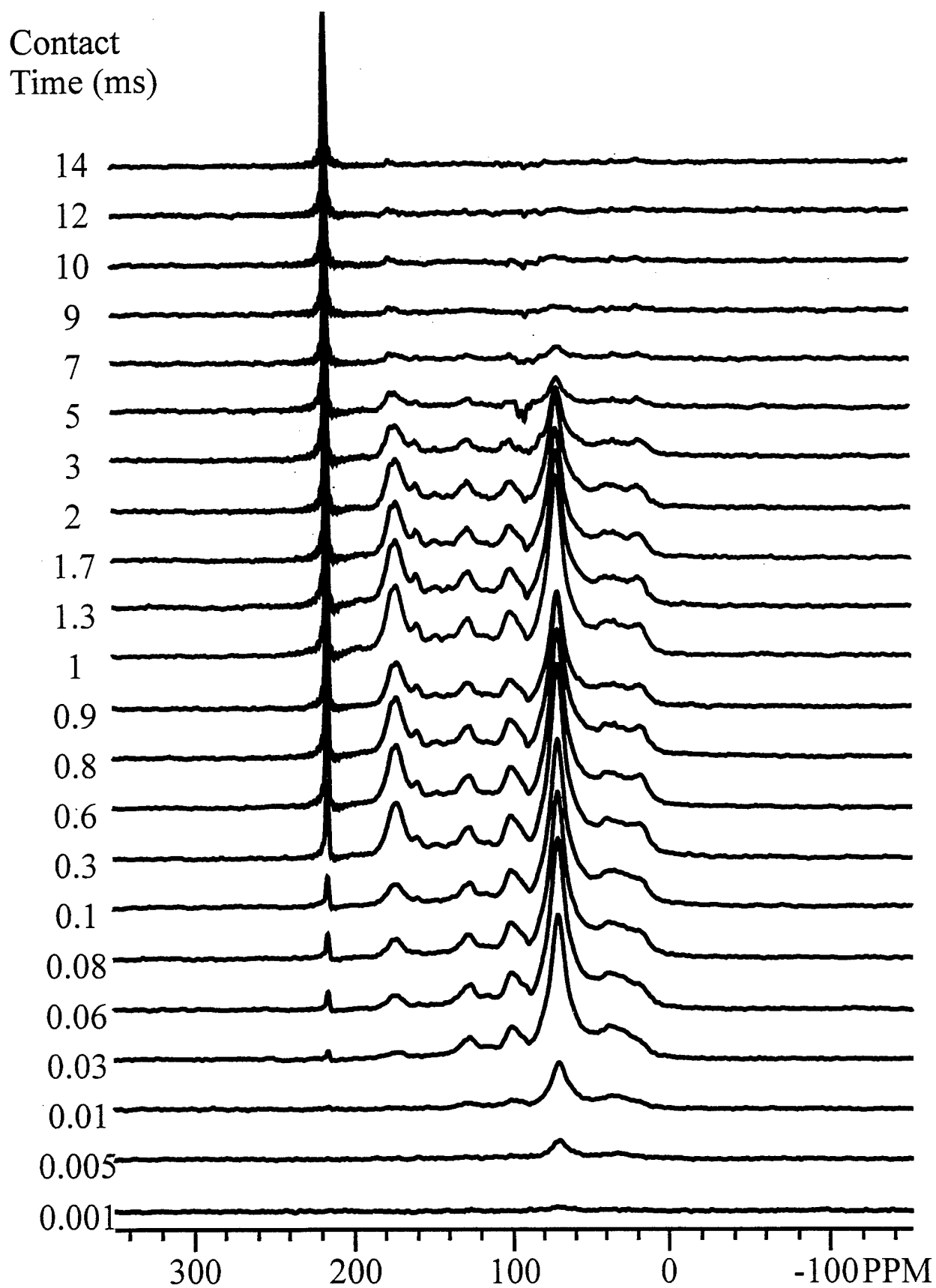


Figure 11. ^{13}C spectra of a variable contact-time CP-MAS experiment on Uncompahgre fulvic acid.

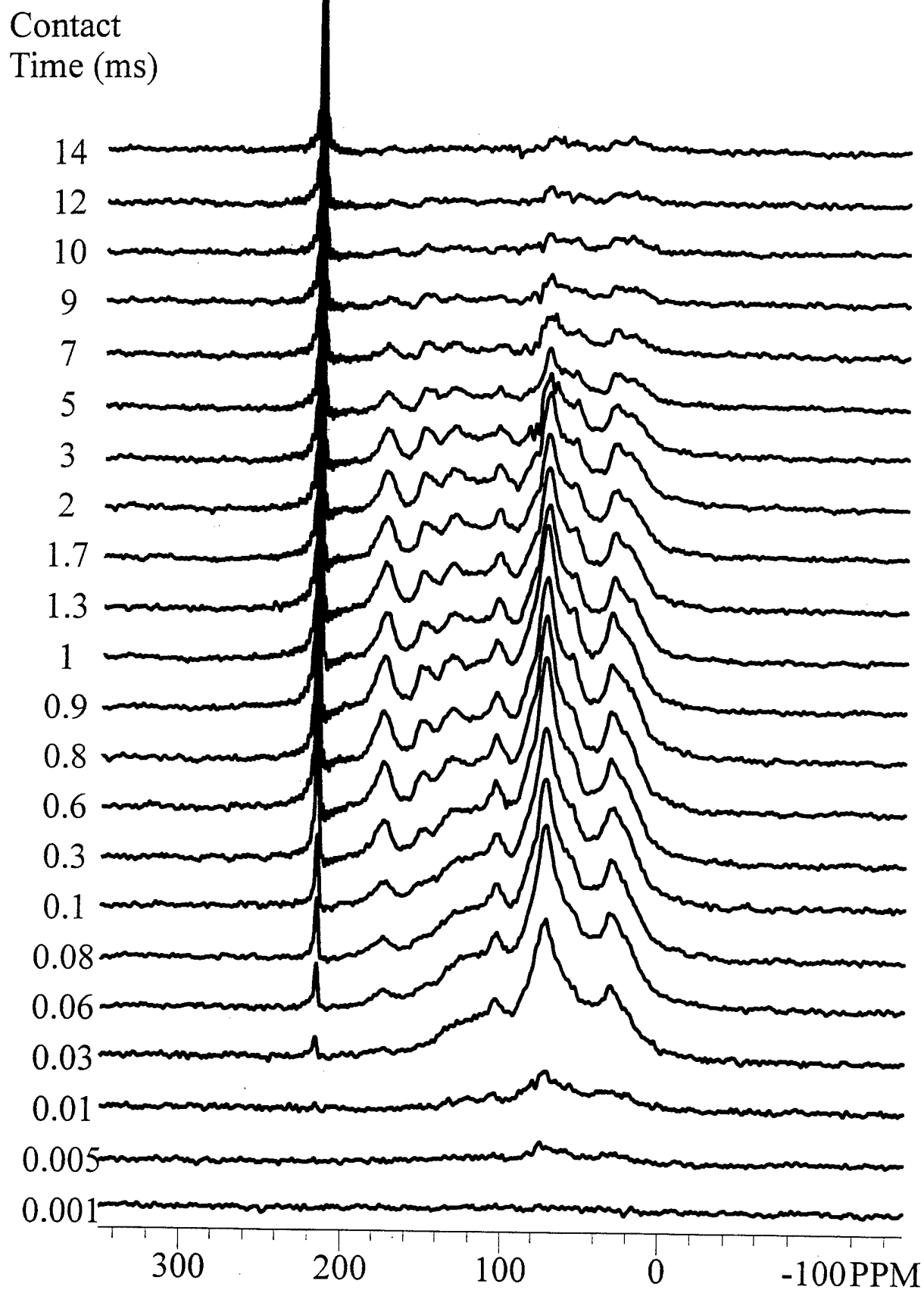


Figure 12. ^{13}C spectra of a variable contact-time CP-MAS experiment on Uncompahgre humin.

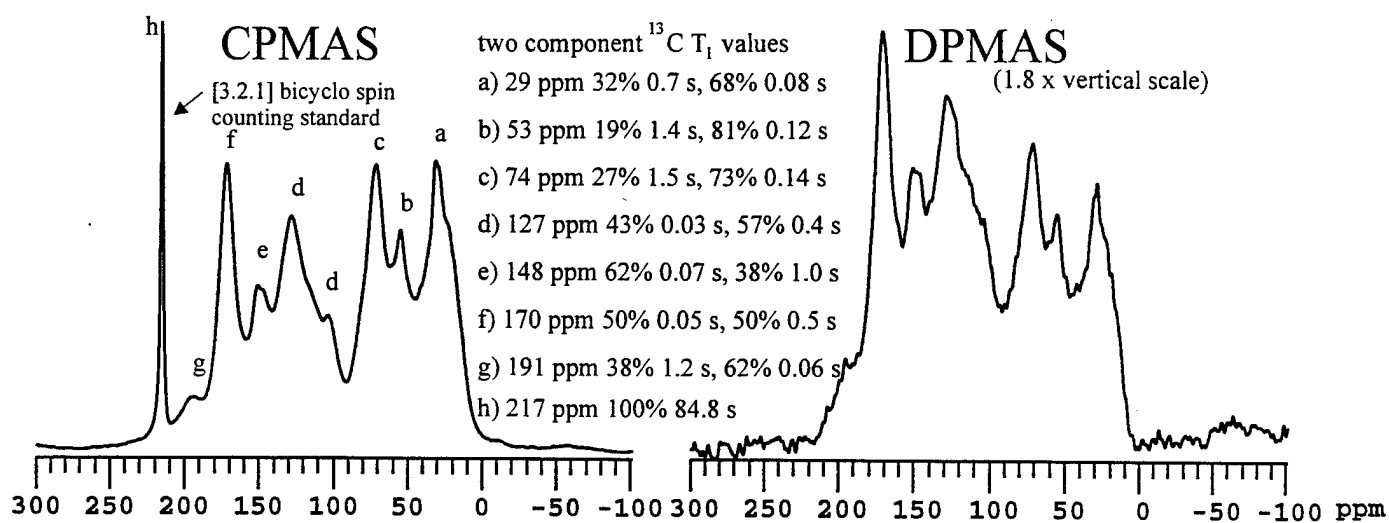


Figure 13. Typical high S/N ^{13}C CP-MAS (A) and DP-MAS (B) spectra of Uncompahgre humic acid, used for ^{13}C spin counting. Intensity reference compound in the sample of A.

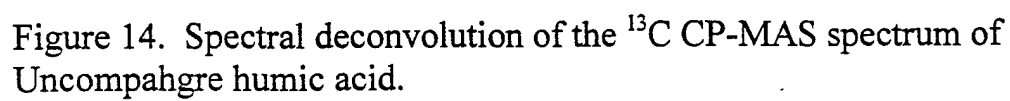


Figure 14. Spectral deconvolution of the ^{13}C CP-MAS spectrum of Uncompahgre humic acid.

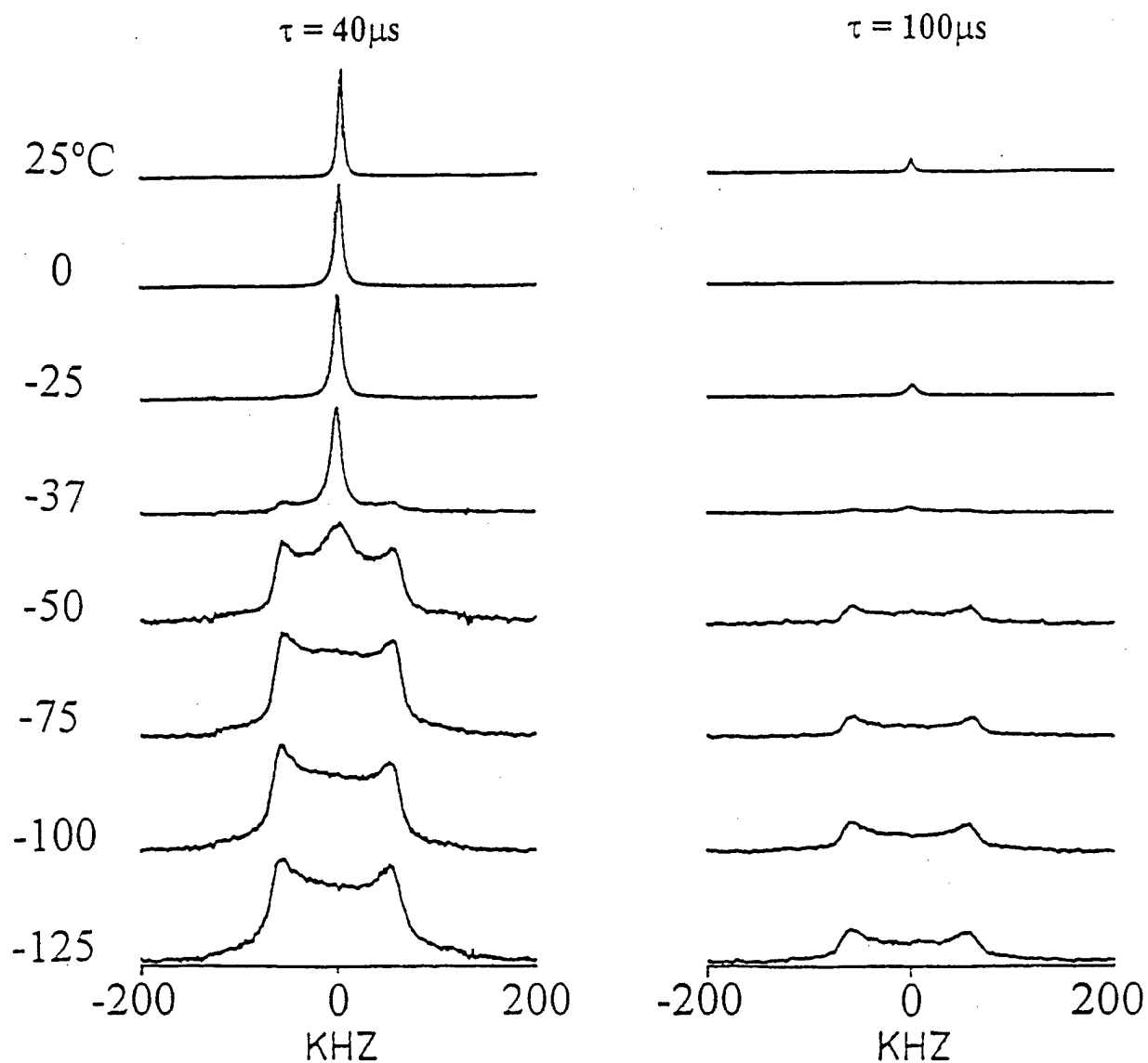


Figure 15. ^2H NMR spectra of $\text{HOCD}_2\text{CD}_2\text{OH}$ adsorbed on Ca-montmorillonite as a function of temperature and quadrupole echo period (τ), as indicated.

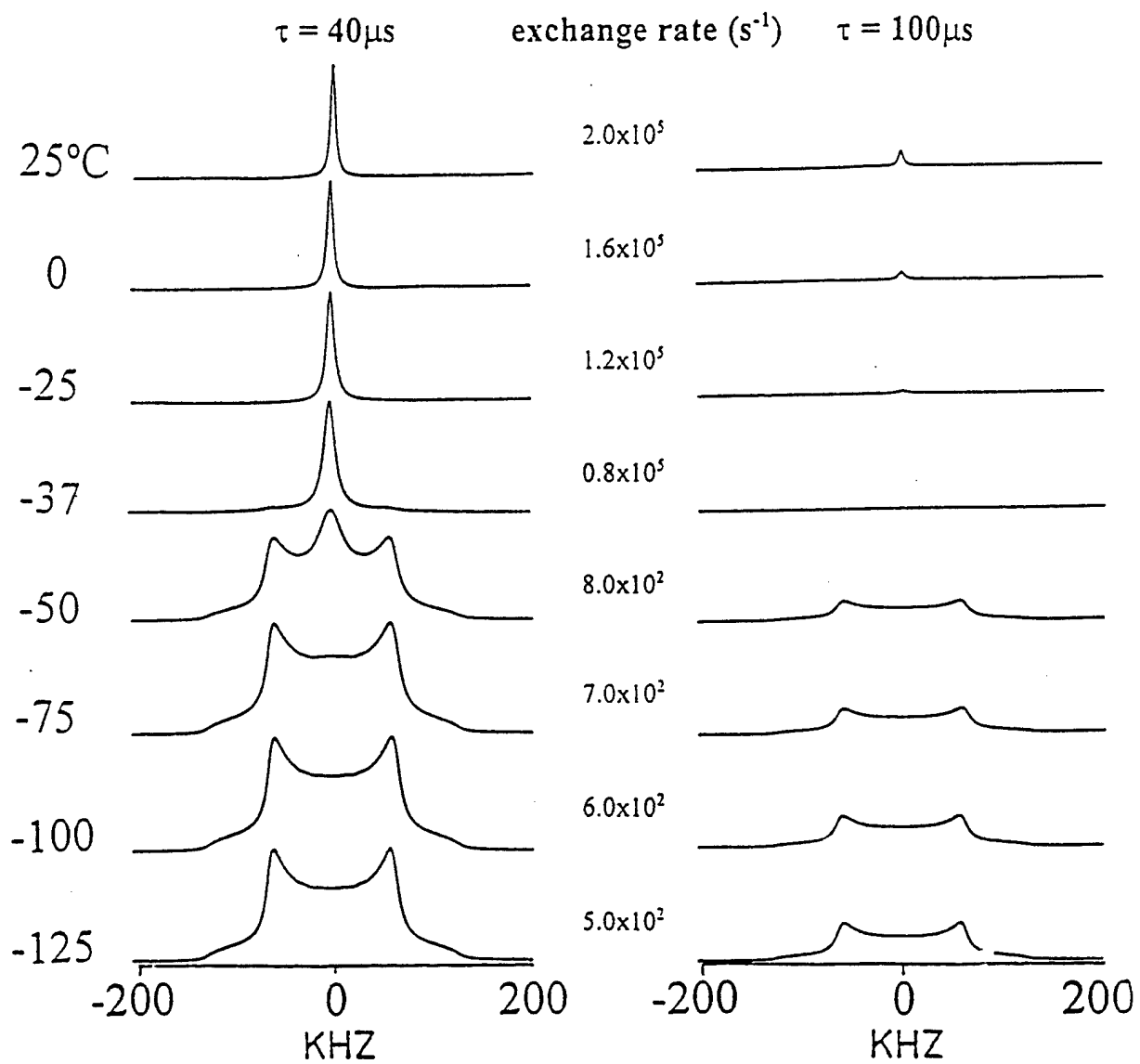


Figure 16. Computer simulations of the ^2H NMR spectra shown in Fig. 15.

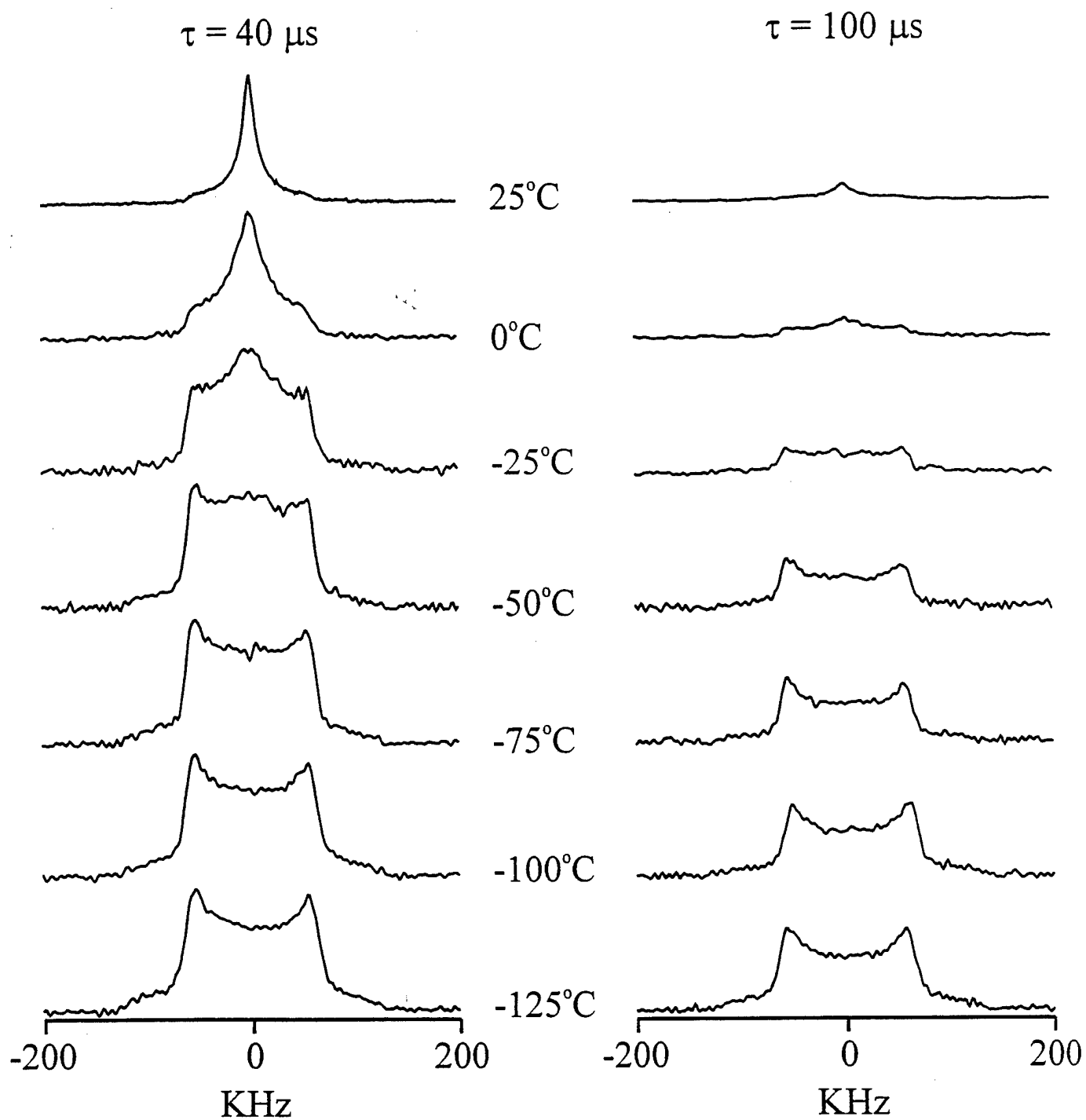


Figure 17. ^2H NMR spectra of a sample of $\text{HOCD}_2\text{CD}_2\text{OH}$ adsorbed on dry Uncompahgre humic acid as a function of temperature and quadrupole echo delay period (τ), as indicated.

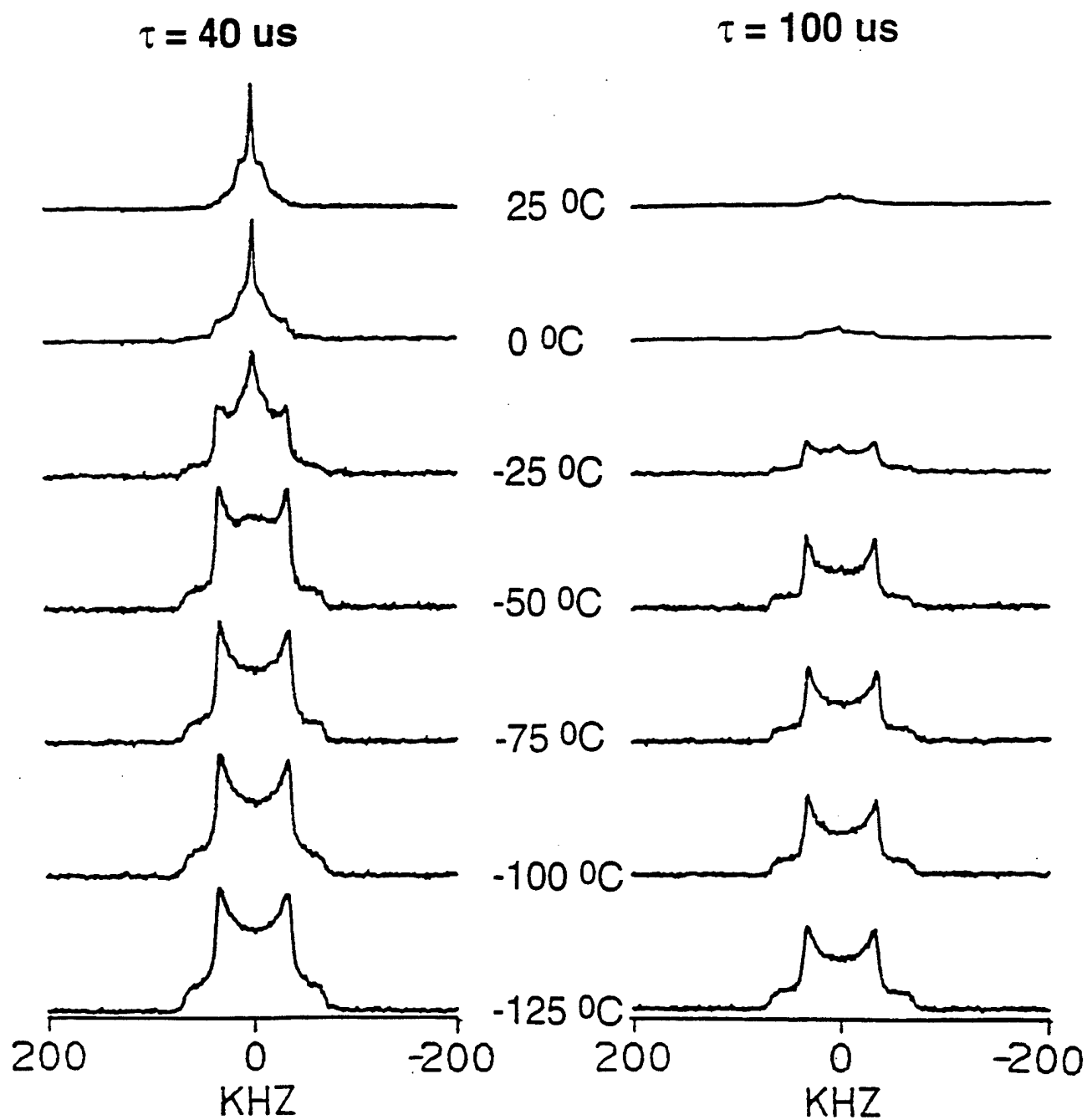


Figure 18. ^2H NMR spectra of a sample of C_6D_6 adsorbed on Ca-montmorillonite (loading level: 1.2 % wt), as a function of temperature and quadrupole echo delay period (τ), as indicated.

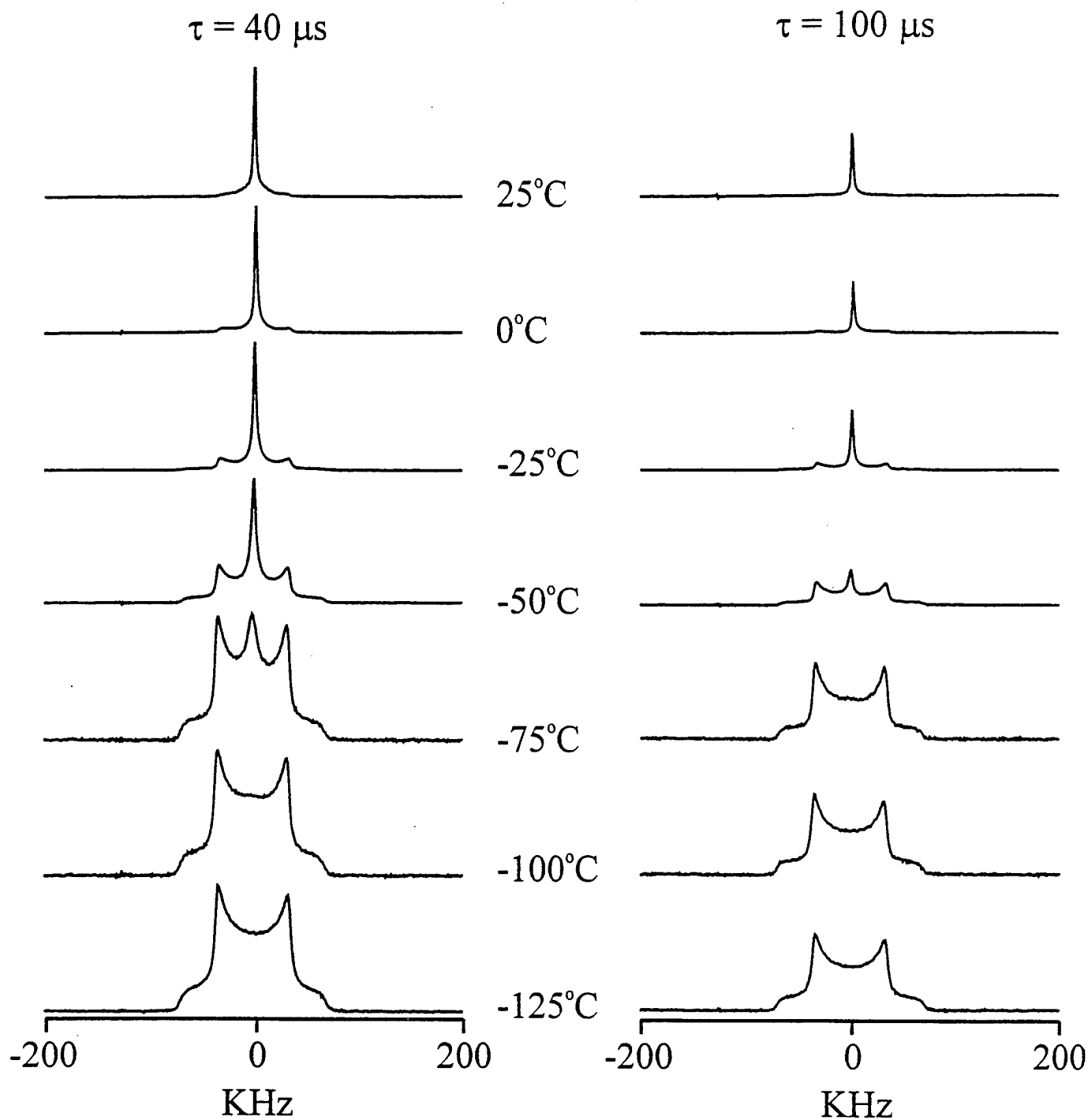


Figure 19. ^2H NMR spectra of a sample of C_6D_6 adsorbed on Ca-montmorillonite (loading level: 3.9 % wt), as a function of temperature and quadrupole echo delay period (τ), as indicated.

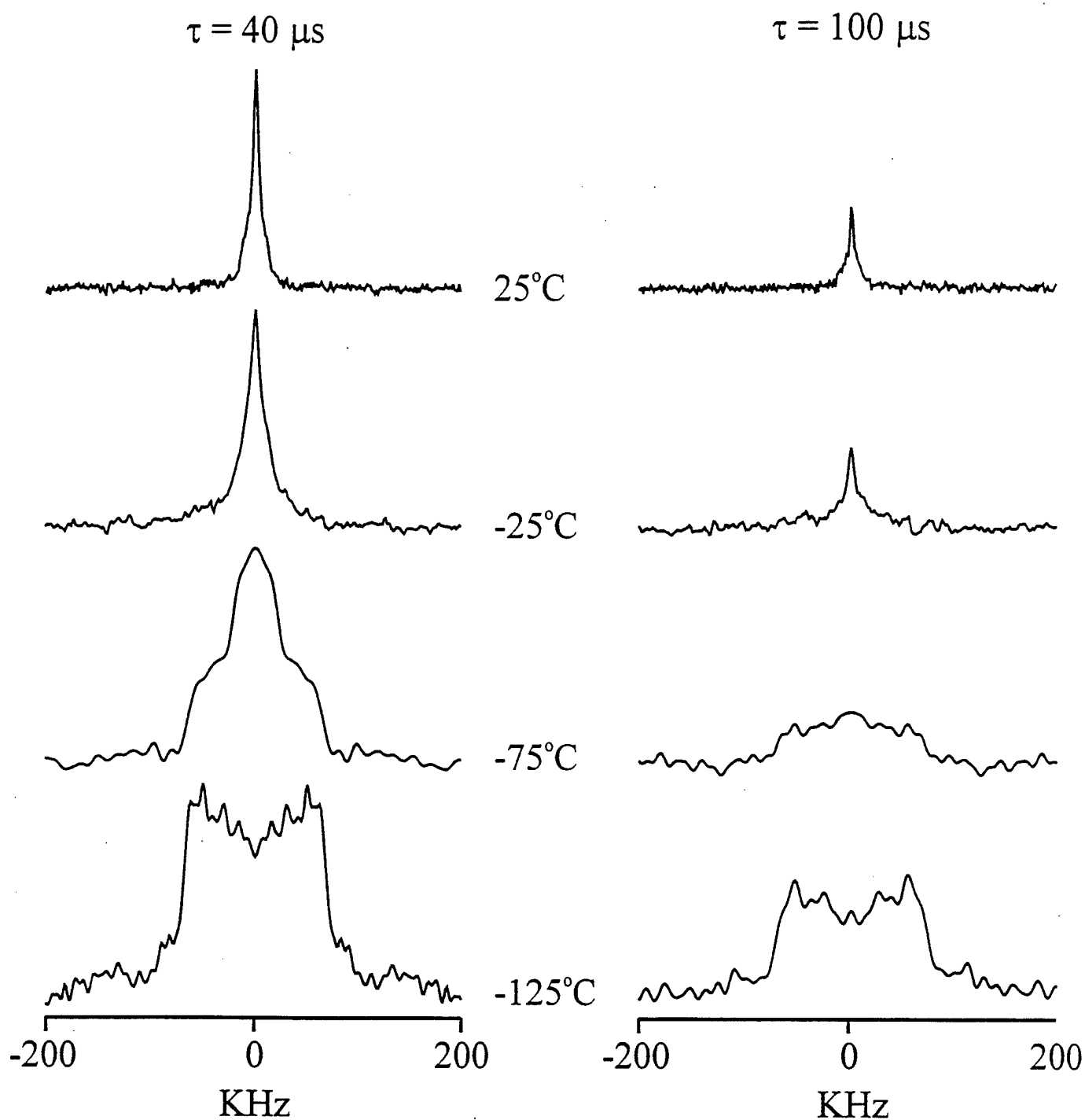


Figure 20. ^2H NMR spectra of a sample of $\text{Cl}_2\text{C}=\text{CDCl}$ adsorbed on Ca-montmorillonite, as a function of temperature and quadrupole echo delay period (τ), as indicated.

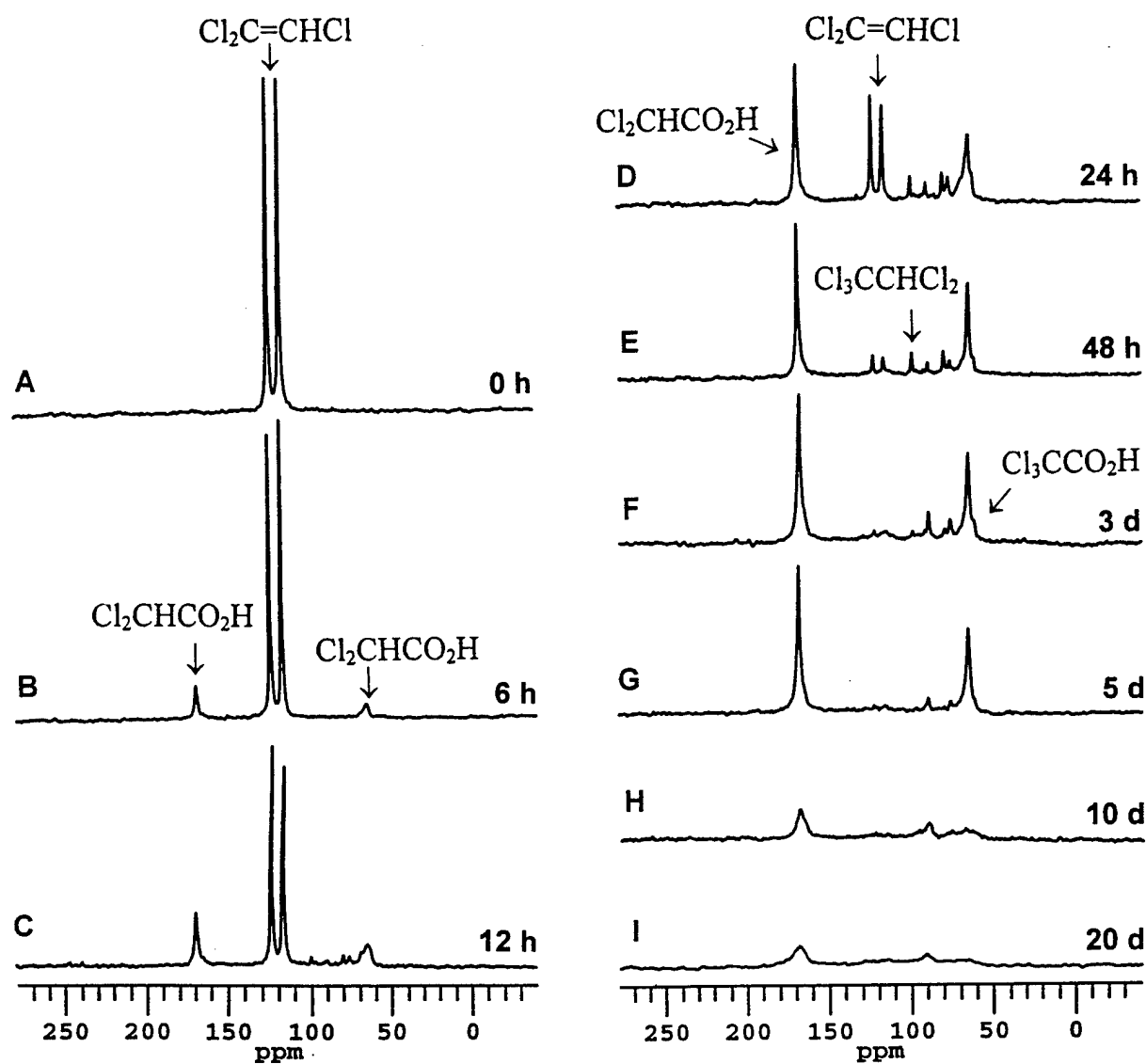


Figure 21. ^{13}C DP-MAS spectra of $\text{Cl}_2\text{C}=\text{CHCl}$ adsorbed on Ca-montmorillonite, subjected to near-UV radiation for various periods of time, as indicated (h = hours, d = days).

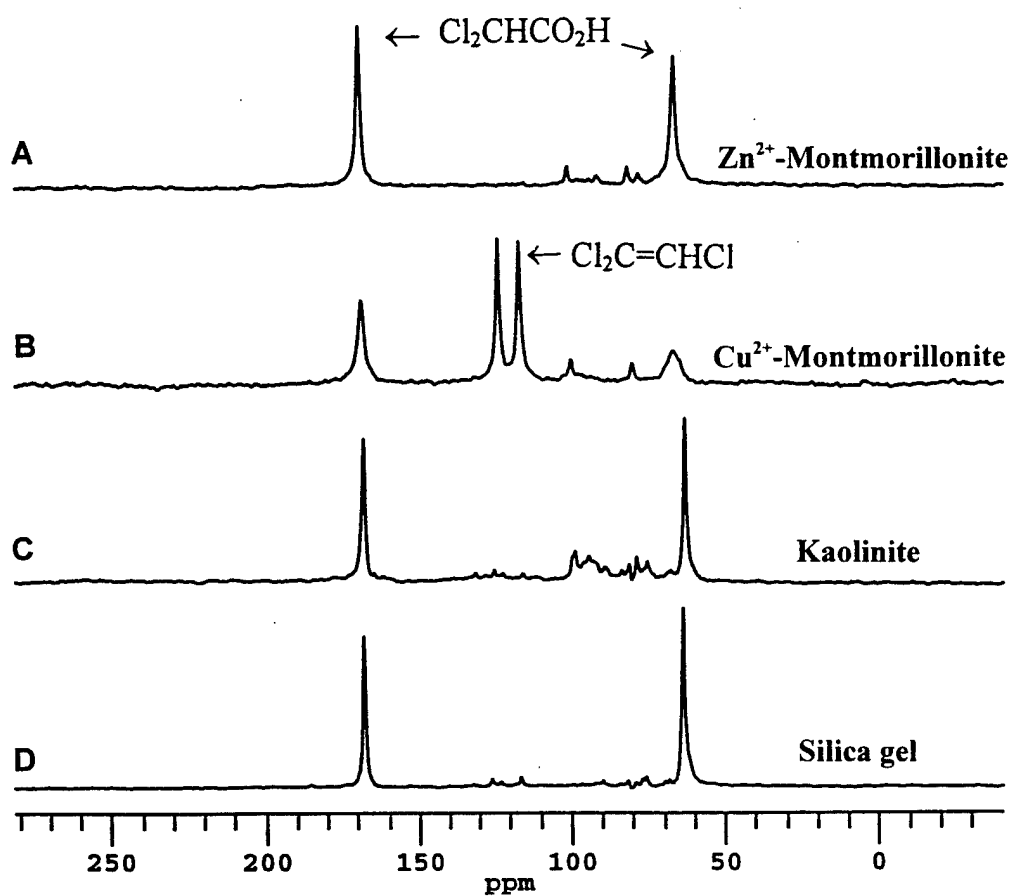


Figure 22. ^{13}C DP-MAS spectra of $\text{Cl}_2\text{C}=\text{CHCl}$ adsorbed on the indicated substrates, subjected to near-UV radiation for 48 hours.

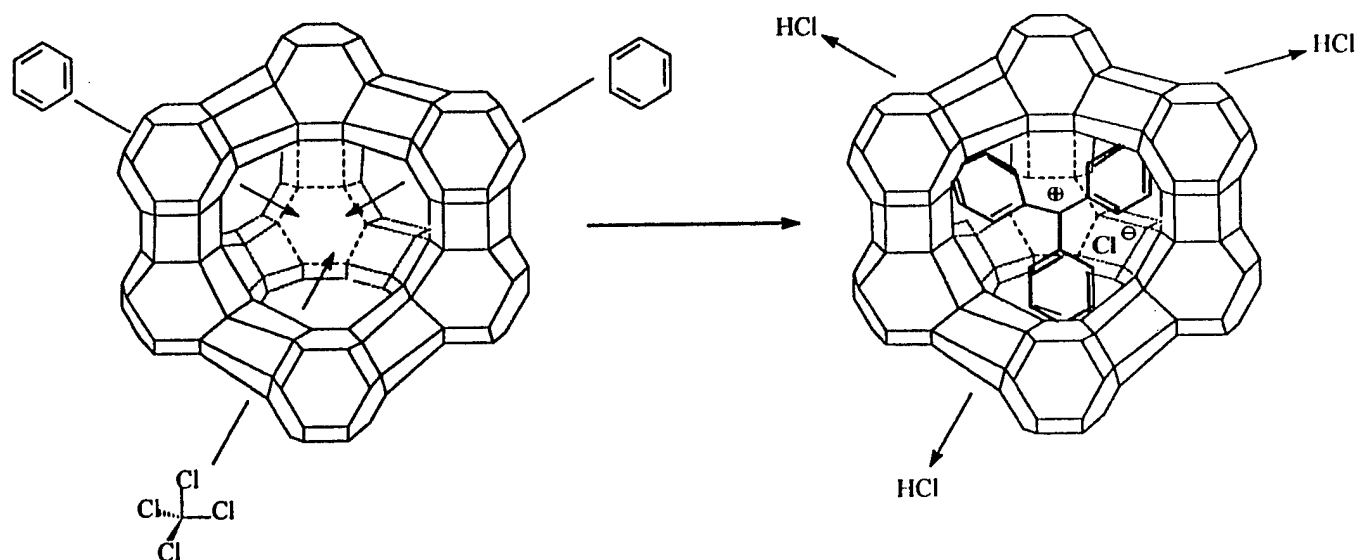


Figure 23. Cartoon representation of the "ship-in-a-bottle" synthesis of $(\text{C}_6\text{H}_5)_3\text{C}^+$ ions inside the cavity of HY zeolite via Friedel-Crafts processes.

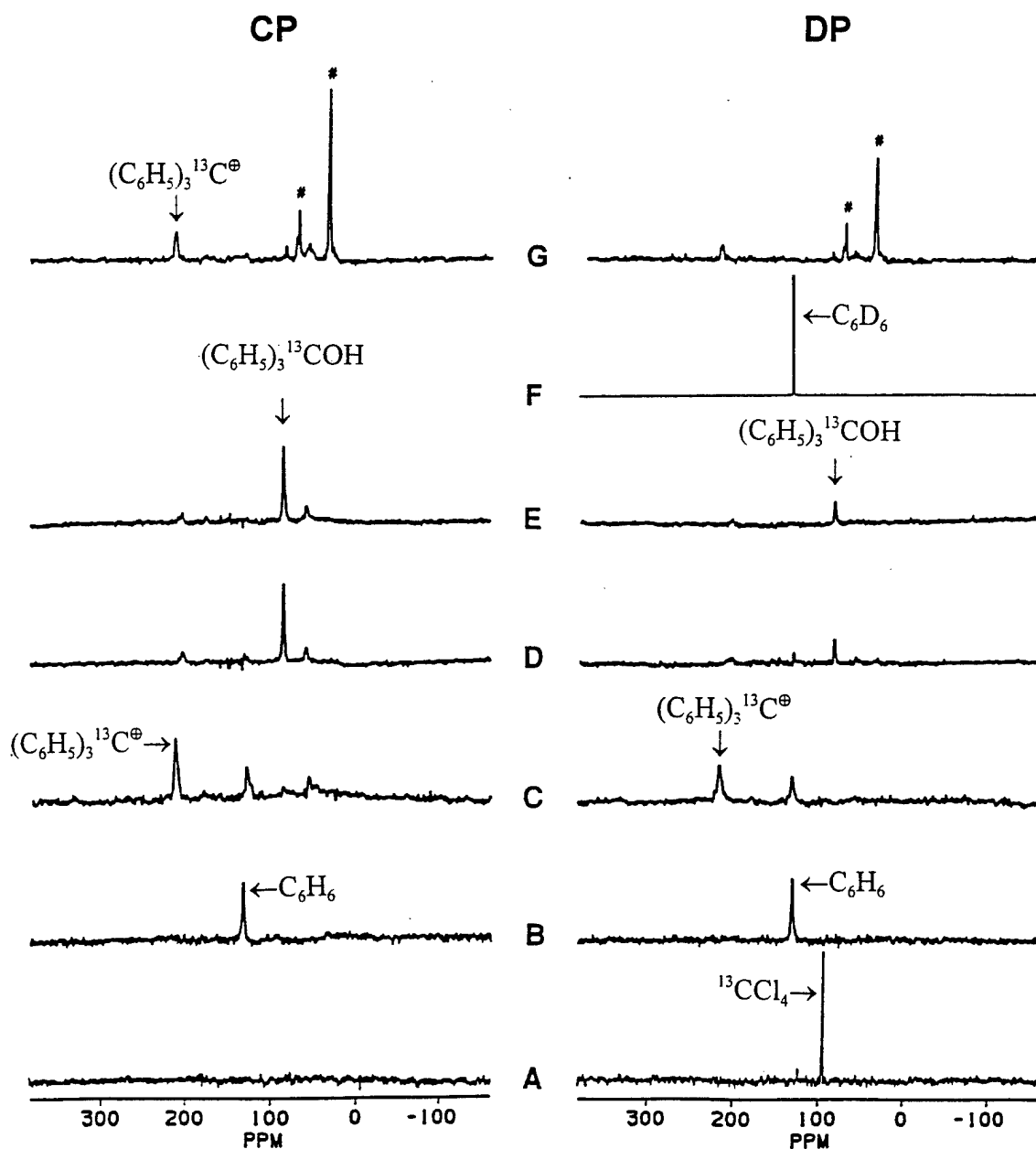


Figure 24. ^{13}C DP-MAS and CP-MAS NMR spectra of the reaction product of $^{13}\text{CCl}_4$ with benzene in HY, and related samples. (A) $^{13}\text{CCl}_4$ mixed with preheated HY; (B) benzene mixed with preheated HY; (C) $^{13}\text{CCl}_4$ and benzene mixed with preheated HY; (D) sample 24C exposed to ambient moisture; (E) solid residue of sample 24D washed with C_6D_6 ; (F) liquid extract from C_6D_6 extraction of sample 24D; (G) product of reaction of sample 24D with $\text{LiAl}[\text{OC}(\text{CH}_3)_3]_3\text{H}$ (peaks marked with # at top correspond to the signals from the reducing agent).

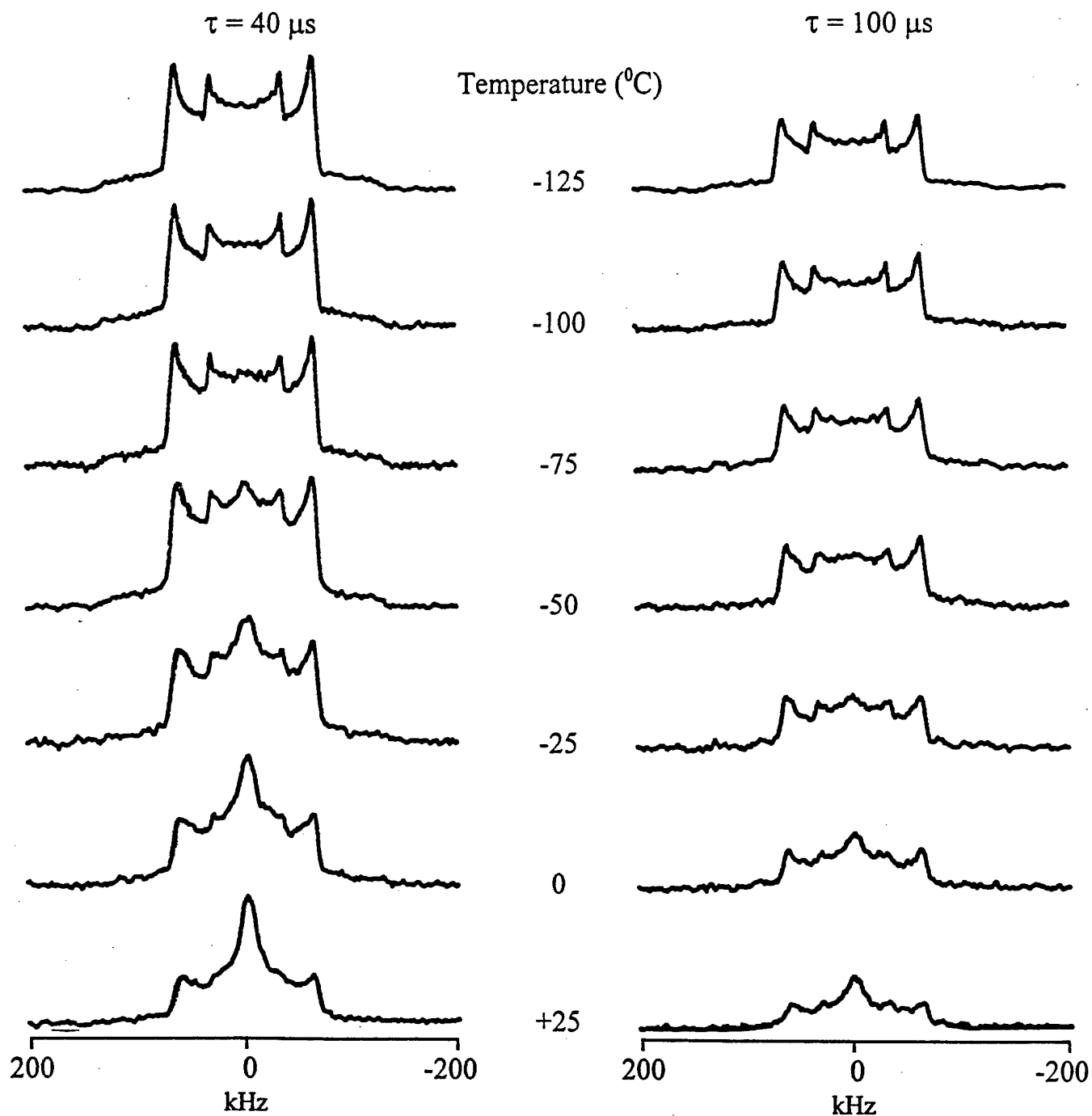


Figure 25. ^2H NMR spectra of $(\text{C}_6\text{D}_5)_3\text{C}^+$ adsorbed primarily in the HY zeolite cavities, as a function of temperature and quadrupole echo delay period (τ), as indicated.

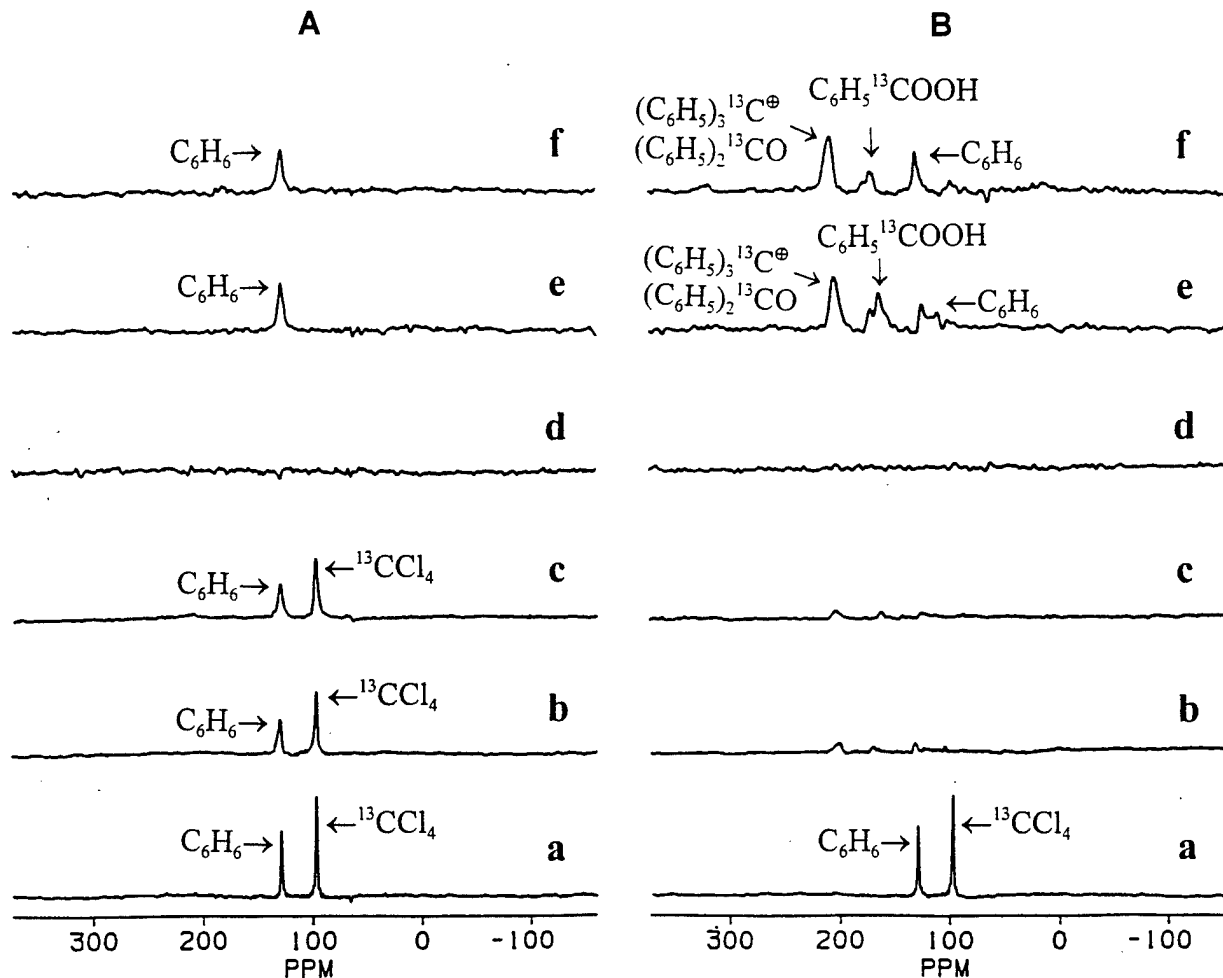


Figure 26. ^{13}C DP-MAS (a,b,c) and CP-MAS (d,e,f) NMR spectra of samples of benzene and ^{13}C -labeled carbon tetrachloride on (A-a, A-d) kaolinite, (A-b, A-e) Ca-montmorillonite, (A-c, A-f) K-10 montmorillonite, (B-a, B-d) Zn^{2+} -exchanged kaolinite, (B-b, B-e) Zn^{2+} -exchanged Ca-montmorillonite and (B-c, B-f) Zn^{2+} -exchanged K-10 montmorillonite.

Final Invention Report

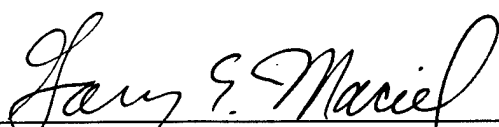
AFOSR Grant F49620-95-1-0192
Organic

"Organic Pollutants in Soils, as Studied by Nuclear Magnetic Resonance"

P.I. Gary E. Maciel

Co-P.I. Willard L. Lindsay

There were no inventions.



Gary E. Maciel

4/20/98

Date